29Si and 27Al MAS NMR spectroscopic studies of activated metakaolin-slag mixtures

Faten Souayfan, Emmanuel Rozière, Michaël Paris, Dimitri Deneele, Ahmed Loukili, Christophe Justino

^{29}Si and ^{27}Al MAS NMR spectroscopic studies of activated metakaolin-slag mixtures

Faten Souayfan[a], Emmanuel Rozière[a], Michaël Paris[b], Dimitri Deneele[b,c], Ahmed Loukili[a], Christophe Justino [d]

[a] Civil engineering and Mechanics Research Institute (GeM), UMR-CNRS 6183, Ecole Centrale de Nantes, 1 rue de la Noe – 44321 Nantes, France

[b] Université de Nantes, CNRS, Institut des Matériaux Jean Rouxel, IMN, F-44000 Nantes, France

[c] GERS-LGIE, Université Gustave Eiffel, IFSTTAR, F-44344 Bouguenais, France

[d] Soletanche-Bachy, Chemin des Processions – 77130 Montereau Fault Yonne, France

Abstract

Blending metakaolin with slag in alkali-activated materials represents a promising way to achieve both acceptable engineering properties and durability. Nuclear Magnetic Resonance (NMR) spectroscopy has appeared as a key technique to investigate the structure of alkali-activation products. However, there is not a consensus on the analysis of NMR spectra to identify the phases formed in binary slag-metakaolin mixtures. This paper characterizes the phase composition and the reaction degree of alkali-activated metakaolin-slag blends, with special emphasis on the effect of H_2O/Na_2O ratio. Different approaches based on the literature are presented and implemented to analyze NMR data. The results suggest the formation of a heterogeneous phase involved in the transformation of 3D network to C-A-S-H. The evaluation of the reaction degree showed that the incorporation of slag in activated metakaolin mixtures resulted in higher reactivity of metakaolin and higher compressive strength.

Keywords

Alkali activated materials, Metakaolin, Slag, Sodium silicate Reaction degree, ^{29}Si MAS NMR, ^{27}Al MAS NMR, Geopolymer, Strength

1. Introduction

Alkali-activated materials (AAM) are considered as a next-generation material to replace Portland cement-based materials for durability purposes in some severe conditions [1]–[4]. They can be obtained by the activation of solid aluminosilicate sources at high pH [5]. Metakaolin and ground granulated blast furnace slag (GGBFS) are the most frequently used materials in AAM production. Ground granulated blast furnace slag (GGBFS) is widely used due to its composition and relatively low cost as an industrial by-product. The main reaction product of the activation of slag is calcium silicate hydrates substituted with aluminum (C-A-S-H) favored by its high calcium content [6], [7]. On the other hand, metakaolin is obtained by the calcination of kaolinitic clays which are considered available enough to meet the demand for building materials [8]. Metakaolin was found more suitable to be used for alkali-activation due to better durability [9]–[13] and possibly lower carbon footprint [14]. Its alkaline activation results in the formation of a geopolymer structure (N-A-S-H) [15]–[17] instead of hydration products with chemically bound water. The development of AAM using blended binders of metakaolin and slag is promising to compensate for the limitation related to each type of precursors. Hybrid metakaolin-slag material has been studied for the last decade [18]–[24]. These binders usually present improved properties compared to systems where metakaolin or slag are activated alone. Only 2% of investigations in recent studies on geopolymer-based materials have focused on binary metakaolin and slag mixtures as reported in [25]. The studies were mainly carried out on concretes and mortars. However, the phase composition was the subject of only a few studies. It was reported that their microstructure includes co-existing Ca-rich and Na-rich reaction products [20], [22]. The presence of geopolymer and slag-based binder in different proportions depending on their composition in a metakaolin-slag material was stated [20] [26]. Other studies mentioned the coexistence of N-A-S-H and N-(C)-A-S-H, both with a 3D network structure, intermixed with C-A-S-H, in

alkali-activated metakaolin-limestone cement [27] [26]. However, there are dispersed opinions describing the phase composition of a hybrid system related to the variety of chemical compositions and amorphous fraction reactivity of the precursors.

Nuclear magnetic resonance (NMR) has become a key tool to study AAM [28]. This method actually allows investigating the local chemical environments regardless of the level of disorder. ^{29}Si and ^{27}Al MAS NMR spectra are usually analyzed to explore the phase composition in alkali-activated materials. The spectral deconvolutions, using appropriate models and constraints, have been used to quantify the reaction products and to calculate the reaction degree [20], [27], [29], [30]. However, the overlap of potential peaks induces ambiguity in their attribution. This puts into question the peak deconvolution methods used in previous works.

The present study aims at investigating the phase composition in binary mixtures using ^{29}Si and ^{27}Al MAS NMR spectra. Different approaches, using ^{29}Si spectra, will be discussed taking into account the different opinions evoked in the literature concerning the present phases and the deconvolution methods. A comparison of different approaches and assumptions, implemented on the same NMR spectra, cannot be found in the literature.

Therefore, the main purpose of this study is to understand the phase composition in binary mixtures by dissecting the different opinions and approaches using ^{27}Al and ^{29}Si MAS NMR spectra. XRD (X-ray diffraction method) was also used to detect the apparition of crystallized phases, if any. A combination of slag and metakaolin at 25% and 75 % respectively has been selected to elaborate the studied materials and they were compared with plain metakaolin mixtures. The influence of H_2O/Na_2O ratio, while maintaining other molar ratios constant, was also investigated. The reaction degree was calculated from the decomposition of ^{29}Si spectra to understand the influence of H_2O/Na_2O ratio and slag incorporation on the compressive strength.

2. Materials and methods

2.1. Materials and sample preparation

The metakaolin used in this study was produced by the flash calcination of kaolin from Fumel, France. It mainly consists of silica (67.1 wt. %) and alumina (26.8 wt. %). The high silica content of metakaolin is due to significant proportion of quartz. Its proportion of pure metakaolin $Al_2O_3(SiO_2)_2$ phase was 43% [31]. The chemical and physical properties of metakaolin and ground granulated blast furnace slag (GGBFS) are described in Table 1.

Table 1. Chemical composition (mass fraction. %) and properties of metakaolin and slag.

(wt.%)	métakaolin	slag
SiO_2	67.1	37.2
Al_2O_3	26.8	10.5
CaO	1.12	43.2
Fe_2O_3	2.56	0.6
MgO	0.11	7.0
SO_3	-	0.1
Cl^-	-	0.01
TiO_2	1.3	0.5
Na_2O	0.01	0.6
Median diameter d_{50} (µm)	18	10
Specific surface BET ($m^2.g^{-1}$)	16.5	0.45
Density	2.63	2.90

The activation solution was prepared by diluting a sodium silicate solution with a fixed SiO_2/Na_2O ratio of 1.7 and 44% dry content in demineralized water. It is noteworthy that the sodium silicate solution was specially designed with relatively high Na_2O content, in order to reduce as much as possible the subsequent addition of NaOH during the preparation of AAMs. A very low sodium hydroxide NaOH content was actually added in pellets to adjust the Na/Al ratio to 1. The molar ratio of SiO_2 to Na_2O in the activator and the chemical compositions have been chosen as recommended in the literature to allow a good dissolution

of the precursor [32]. Therefore, the total NaOH content in activating solution includes equivalent NaOH from the sodium silicate solution deduced from its Na_2O molar content, and NaOH in pellets. The alkali-activated mixtures were designed to obtain the stoichiometry of the systems detailed in Table 2. Molar ratios were calculated considering the initial chemical composition of the sodium silicate solution, added NaOH, the amorphous fraction of the metakaolin, and slag. Activated metakaolin systems have been designed with constant Si/Al, Na/Al atomic ratios and different H_2O/Na_2O molar ratios.

Table 2. Compositions of the studied mixtures

Mixtures		**MK21**	**MK34**	**MKS21**	**MKS34**
Materials	**Density**	**Compositions (g/l)**			
Metakaolin	2.63	732	518	562	397
Slag	2.9	-	-	187	133
Na-silicate	1.55	636	450	636	450
NaOH pellets	1.46	3.3	2.3	3.3	2.3
Bentonite	2.5	9	15	9	15
Dispersant	1.4	5.5	4	5.5	4
Water	1	310	511	310	511
Water to solid ratio (W/S %wt.)		0.65	1.04	0.65	1.04
Volume fractions (%)					
Water		66	76	66	76
Solid phases		34	24	34	24
Atomic ratios					
Si/Al		1.83	1.83	2.20	2.20
Na/Al		1	1	1.1	1.1
Molar ratio					
H_2O/Na_2O		21	34	21	34
Total NaOH in activating solution (mol/l solution)		5.29	3.25	5.29	3.25

Binary metakaolin-slag mixtures were derived from 100% metakaolin mixtures. Metakaolin was replaced by 25 %wt of slag at constant volume. The water to solid ratio is calculated from the total water in the mixture, including the added demineralized water and the water fraction in the activation solution, and the total amount of solid including the precursor and the solid fraction of the activation solution. The total NaOH in activating solution takes into account NaOH from the sodium silicate solution and added NaOH pellets. The total NaOH concentration decreased with water-to-solid ratio but remained relatively high. Based on a previous study [33], bentonite and dispersant were added for the stabilization and deflocculation of particle suspensions respectively. Regarding the mixing procedure, the powders were added to the activating solution and stirred in a high shear mixer for 5 minutes to ensure a proper homogenization. The specimens characterized at hardened state were sealed and stored at 20°C.

2.2.Test methods

2.2.1. Compressive strength

The compressive strength testing was carried out on a 100kN press. The load rate was 1.9kN/s until failure. Compression tests were performed at the ages of 7, 28 and 90 days on cylinders with a diameter of 7 cm and a height of 14cm.

2.2.2. Nuclear magnetic resonance (NMR)

Solid-state ^{29}Si NMR spectroscopy was performed using a Bruker Avance III 300 MHz (7 T) spectrometer and a 7mm MAS probe, and ^{27}Al magic angle spinning (MAS) NMR spectroscopy was performed on a 500 MHz Bruker Avance III using a 2.5mm MAS probe. For ^{27}Al acquisition, the MAS speed was 30 kHz and the repetition time was set to 1s. The ^{27}Al spectra were carried out with a single $\pi/13$ excitation pulse for a radiofrequency field of 12 kHz. Chemical shifts were referenced against $Al(NO_3)_3$ solution. For ^{29}Si acquisition, the

MAS speed was 5 kHz. The ^{29}Si MAS NMR spectra were acquired with single $\pi/2$ excitation of 5.5 µs. The recycle delay between scans was set to 5s. Chemical shifts were referenced against TMS.

2.2.3. X-ray diffraction (XRD)

XRD is mainly used to describe crystallized phases. Geopolymers are mainly amorphous so XRD is relevant to investigate the consumption of primary alumino-silicate phases and to detect the apparition of new crystallized phases. The X-ray diffractograms were obtained from a Bruker AXS D8 Advance diffractometer, equipped with an anticathode tube made of copper (Cu-Kα : λ = 1.5418 Å). Voltage and current were set to 40 kV and 40 mA. Disoriented powders diffractograms were recorded between 2°2θ et 60°2θ with a step equal to 0,017°2θ and a measuring time of 1 second per step. Diffractograms were analyzed thanks to EVA software from Bruker and the Crystallography Open Database.

3. Results and discussion

3.1. Mechanical properties

Figure 1 shows the compressive strength development of activated metakaolin and activated metakaolin-slag mixtures at 7, 28, and 90 days respectively. The binary mixtures developed significantly higher strength than plain metakaolin system at the same H_2O/Na_2O ratio. This is consistent with previous results reporting that adding slag to activated metakaolin has a positive effect on the development of mechanical strength [21] [23]. A drop in strength can be observed when increasing H_2O/Na_2O ratio to 34 in both activated metakaolin and metakaolin-slag mixtures. The compressive strength of MK21 was around 19 MPa after 90 days whereas the strength of MK34 was still not measurable. Increasing H_2O/Na_2O leads to lower strength and higher porosity as water affects density and open porosity [34] [35]. Additionally, the composition and the structure of the reaction products can be changed depending on the

amount of water available in the system and the concentration of alkali cations [29], [36], [37] but the experimental data related to the effect of water with constant molar ratios are scarce.

Compressive strength of studied mixtures increased from 7 to 90 days. This can be attributed to reaction advancement and/or microstructure evolutions. Chen et al. [38] quantitatively correlated the degree of reaction related to the amount of gel formed with the compressive strength of metakaolin-based geopolymers with and without calcium. Cherki El Idrissi et al. [16] showed that the mechanical properties of metakaolin-based materials highly depend on the changes in local structures. However, it is still not clear how slag and water content modify the reactivity of precursors and the structure of formed products. X-ray diffraction was used to analyze the formation of crystalline materials if any. Additionally, the local structure was investigated for all mixtures using ^{29}Si and ^{27}Al NMR spectroscopy to understand the effect of H_2O/Na_2O ratio and slag incorporation on binding phase and to estimate the reaction degree at different curing times.

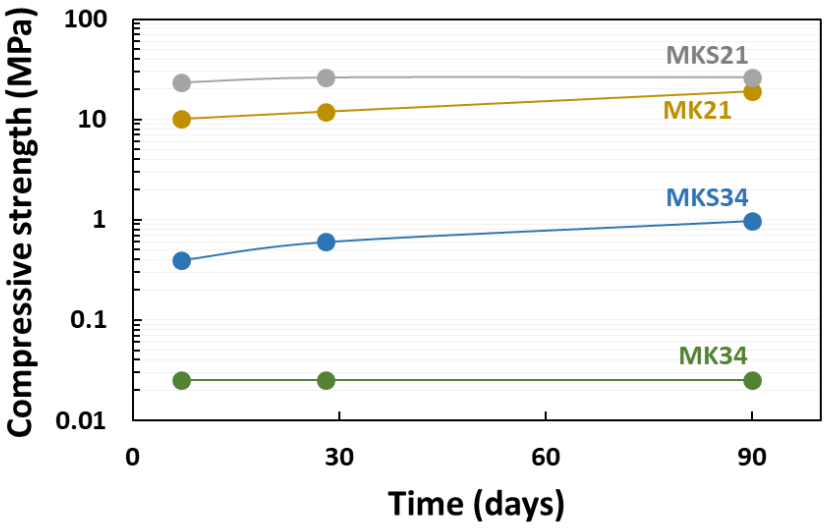

Figure 1. Compressive strength development of different mixtures at 7, 28 and 90 days

3.2. Phase composition

3.2.1. X-ray diffraction (XRD)

Figure 2 represents the XRD patterns of different mixtures at different ages. The major crystalline phase is quartz (SiO_2) originating from raw metakaolin. The carbonation of slag hydration products in binary mixtures can contribute to calcite formation. Calcite could be detected in MK21 at 28 days despite the low Ca content in metakaolin. Anatase (TiO_2) and kaolinite $Al_2Si_2O_5(OH)_4$ observed in all samples originated from the raw materials.

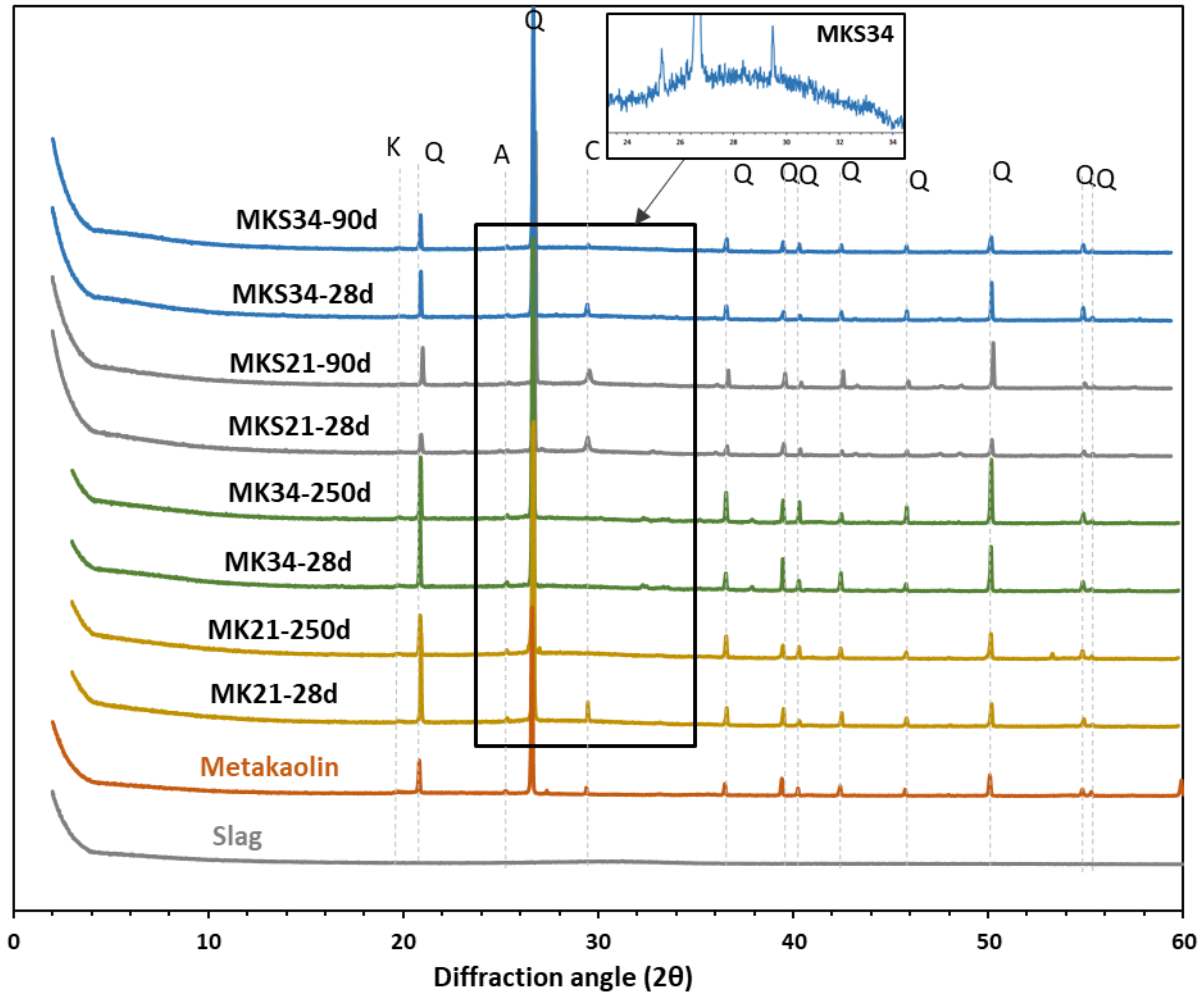

Figure 2. XRD patterns of different mixtures,

C: calcite; Q: quartz, A: Anatase, K: Kaolinite

New crystalline products could not be detected except calcite. A broad hump can be observed between 2θ=25° and 2θ=35°. This implies that all the products, which are specific to reactions involving sodium silicate, metakaolin and slag, are very poorly crystalline. This hump in such mixtures is often associated with the geopolymer products [39] whose crystalline domains can be of about 5 nm [27], which is below the detection limit of XRD. It is noteworthy to mention that adding slag to the mixtures did not result in the formation of new crystalline phases. However, the hump at 2θ=30° can be attributed to an aluminum substituted tobermorite-like phase ($Ca_5Si_5Al(OH)O_{17}.5H_2O$,) [7]. This phase is expected to be formed in such mixtures [16], [22], [26], [30], [40]. It is although mostly amorphous and can be integrated into the amorphous hump mentioned above.

3.2.2. ^{27}Al NMR analyses

^{27}Al NMR spectra of the raw metakaolin and activated mixtures cured for 28 and 250 days are presented in Figure 3. Raw metakaolin exhibits three overlapping peaks with maxima at 55 ppm, 28 ppm, and 4 ppm according to four, five, and six-coordinated aluminum, respectively. The width of these peaks reflects the amorphous character of the metakaolin attributed to dehydroxylated kaolin. The slag spectrum shows broad overlapping peaks attributed to a variety of aluminum environments with a majority of Al(IV). All activated mixtures spectra showed a main resonance with a maximum between 58 and 60 ppm that corresponds to tetrahedral sites AlO_4(4Si) type in aluminosilicate glasses [41]. The variation of H_2O/Na_2O did not significantly influence the position of the main resonance peak in both types of mixtures.

In the activated metakaolin systems, the predominant signal centered around 58 ppm corresponds to tetrahedrally coordinated aluminum in the reaction products forming a three-dimensional silico-aluminate framework, in agreement with previous observations of

aluminosilicate-based geopolymers [15], [42], [43]. Significant spectral intensity below 40 ppm (Al^{V} and Al^{VI} signals) indicates that a higher amount of metakaolin did not react at higher H_2O/Na_2O.

Small variations in the shielding of the resonances are observed by comparing binary metakaolin-slag systems to activated metakaolin mixtures. The ^{27}Al chemical shifts may be affected by geometric factors such as T-O-T angles (where T is Si or Al) or the type of cations in more distant coordination spheres [29] [44]. Walkley et al. [44] reported that the incorporation of Sr^{2+} and Ca^{2+} at a low concentration displaces some of the alkali cations Na^{+} and K^{+} from the extra-framework sites and fulfill the charge balancing role. It was found that adding calcium to the metakaolin system results in a slight shift from 56.6 ppm to 57.9 ppm in ^{27}Al NMR spectrum [45]. Ca^{2+} can be taken up in the 3D aluminosilicate network and compensate the negative charge after the replacement of Si^{4+} by Al^{3+} [45]. The incorporation of slag in the system also resulted in a slight increase in the full width at half height (FWHH). This observation is consistent with a recent study reporting an increase in the FWHH of the AlO_4 resonance as the calcium content increases in the mixtures can be explained by the higher Ca^{2+} uptake in the aluminosilicate structure [27].

Nevertheless, Bernal et al. [46] mentioned that the resonance in fly ash–slag mixtures, which is somewhat broader than solely fly ash, is comprised of a contribution at a high chemical shift from the C-A-S-H gel and another at a lower chemical shift from the N-A-S-H gel. Both phases would contain Al in significantly distorted tetrahedral environments, which lead to the broad resonance centered around 58 ppm [46] [40].

In our study, binary mixtures and plain metakaolin systems showed a slight difference in the position, shape and width of ^{27}Al spectrum. Further information on the short-range order of the silicate tetrahedral is presented in the following section.

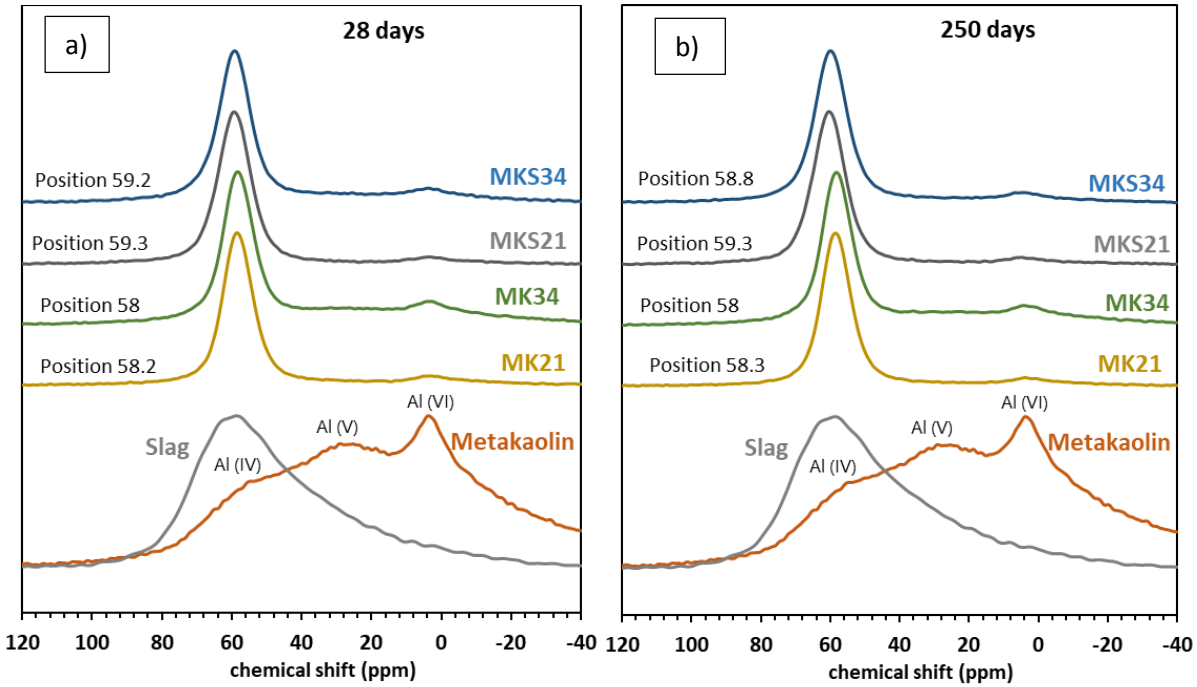

Figure 3. ^{27}Al MAS NMR spectra of raw metakaolin, raw slag and activated systems at 28 and 250 days

3.2.3. ^{29}Si NMR analyses

Figure 4 shows the ^{29}Si MAS NMR spectra of the raw metakaolin, raw slag, and sodium silicate activated mixtures. The broad asymmetric resonance width is indicative of the amorphous structure of these materials. Raw metakaolin spectrum presents a main peak with a maximum at -99 ppm. The peak detected at -107 ppm comes from the quartz present in raw metakaolin [16]. The spectrum of raw slag lies in a variety of Q^0, Q^1, and Q^2 sites, mostly Q^0 resulting in a peak maximum around -75 ppm.

Activated metakaolin systems presented a broad resonance with a maximum between -91 ppm and -93 ppm regarding H_2O/Na_2O ratios. A shift of the overall ^{29}Si spectra to lower frequencies is observed at high H_2O/Na_2O ratio. However, this resonance in the ^{29}Si spectra is mainly attributed to the Q^4 type environment and its width is explained by the presence of the Q^4(mAl) type environment with m varies between 0 and 4 [16] [42]. This is in accordance

with the observed ^{27}Al spectrum (Figure 3) where the large peak centered at 58 ppm comes from the four-coordinated aluminum Al (IV) in geopolymer structure. In agreement with previous section, the shoulder in resonances at about -100 ppm, more intense in the mixture with higher H_2O/Na_2O ratios, confirms the remnant metakaolin in the activated metakaolin systems at 28 and 250 days (detailed in the following section). The residual quartz present in raw metakaolin can be also detected at -107 ppm.

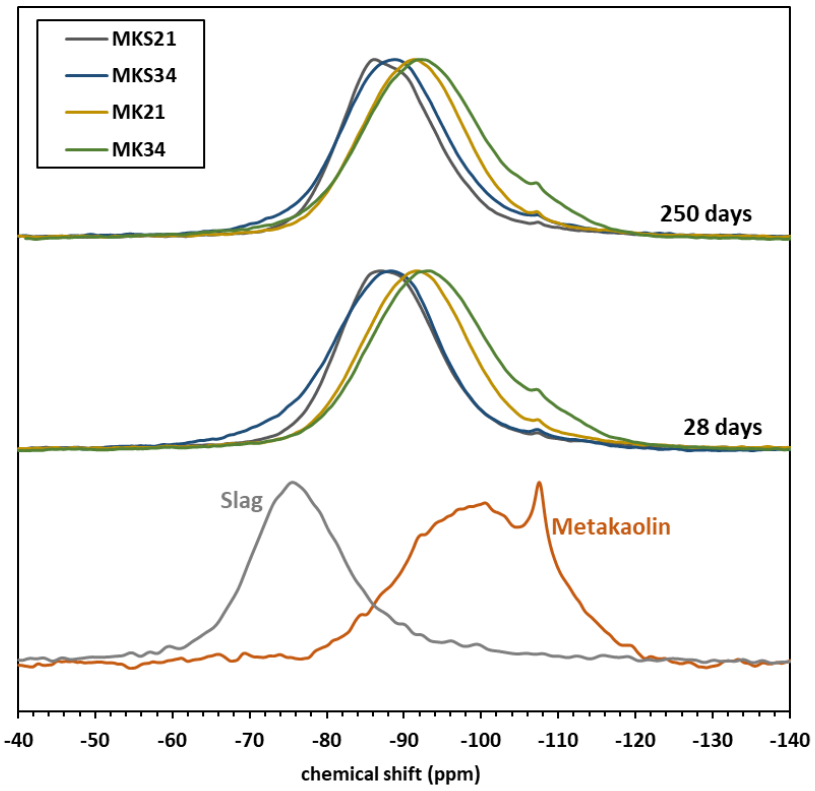

Figure 4. ^{29}Si MAS NMR spectra of raw metakaolin, raw slag and activated systems

In binary mixtures, spectra shifted to higher frequencies in comparison with plain metakaolin mixtures (between -72 ppm and -110 ppm). The main resonance peaks between -91 ppm and -93 ppm observed in plain metakaolin mixtures shifted to -87 ppm and -89 ppm. The ^{29}Si spectrum of the mixture MKS34 shifted to slightly higher frequencies than the mixture MKS21, probably due to the remnant metakaolin. It is noteworthy to mention that after 250 days, the intensity of the shoulder observed at -76 ppm in the mixture MKS34 decreased,

implying a further dissolution of slag in function of the time. A sharp peak in MKS21 after 250 days appeared at -86 ppm. This can indicate a structural organization of the product phase with curing time.

The broad width, in binary mixtures, indicates the presence of Si in different environments of type Q^n(mAl), where n is the coordination number of the silicon center and m is the number of aluminum atoms neighbors ($0 \leq n \leq m \leq 4$). Based on the literature, chemical shifts between -75 ppm and -94 ppm can be referred to Q^1, Q^2, Q^2(1Al), Q^3(1Al), and Q^3sites in an Al substituted C-S-H type (C-(A)-S-H) gel with a tobermorite type structure [16]. These sites can overlap with Q^4 type environment (often detected between -88 ppm and -109 ppm [16] [42]) with Al uptake by the alkali-aluminosilicate gel network expected to be formed in such mixtures. Different studies concluded on the presence of two distinct intermixed gels in activated blends [30] [22]. Buchwald et al. [20] reported the presence of geopolymer and hydrated slag binder in different proportions depending on their composition in a metakaolin-slag material.

On the other hand, the coexistence of N-A-S-H and N-(C)-A-S-H, both with a 3D network structure, intermixed with C-A-S-H have been identified in alkali-activated metakaolin-limestone cement [27]. This observation is in agreement with the results on the calcium metakaolin activated system evoked in [38] [26] [45]. The simultaneous presence of C-A-S-H with a 2D structure and Q^1 and Q^2 sites, intermixed with a calcium modified geopolymer gel that has 3D structure with Q^3 and Q^4 sites, and with an aluminosilicate gel N-A-S-H with Q^4 sites were identified in [38] [26]. Adding calcium to an aluminosilicate system resulted in an uptake of calcium into N-A-S-H gel with a preserve of the 3D structures [44] [45]. It was suggested that Ca^{2+} uptake into N-(C)-A-S-H happens through an ion-exchange mechanism in which Ca^{2+} displaces Na^+ after the formation of N-A-S-H [17] [27]. The transition from a 3D structure towards a linearly structured one depends on the availability and form in which the

Ca, Na, Si, and Al are supplied [27]. Lodeiro et al. [17] have proposed a model for the stability of N-A-S-H gel as function of pH and Ca concentration.

Based on this, intermixed gels can be expected in the studied materials. It is noteworthy to mention that the identification of the coexisting phases and their respective proportions are key data to understand their macroscopic properties, such as strength and durability. The reaction products formed in this experimental study are discussed in detail in the following section by taking into account the dispersed opinions discussed the role of calcium. The results related to a set of initial assumptions allow discussing their relevance. ^{29}Si spectra have been deconvoluted using Dmfit free software to perform spectral simulations [47]. Therefore, a quantification of the resonance species have been achieved and the reaction degree of metakaolin and slag and the overall degree of reaction have been then calculated to understand the effect of both slag incorporation and H_2O/Na_2O ratio on the reaction advancement and the phase composition.

3.3. Towards the quantification of reaction products

The ^{29}Si spectra are deconvoluted using a series of Gaussian peaks to simulate resonances using a least-square fitting method which is routinely performed in the study of alkali-activated materials. In all spectra deconvolutions, congruent dissolution of slag and metakaolin is assumed [44] [20]. The contribution of the remnant metakaolin is considered by fitting a scaled component spectrum calculated from the ^{29}Si MAS NMR spectrum of raw metakaolin and raw slag, respectively. Raw metakaolin is represented by a Gaussian signal centered at -99 ppm. The contribution of quartz around -107 ppm has not been considered because of the very long relaxation delays associated with the Q^4 sites in quartz which means that they will not be captured quantitatively in the spectra here. Additionally, the quartz reactivity is neglected thus it is not taken into account in the advancement of the reaction.

Three approaches are used to analyze and quantify the reaction products and the remnant precursors (Table 3). The Gaussian lines used for the decomposition of ^{29}Si spectra are usually defined by their intensity, the peak position, and the full width at half height (FWHH).

Table 3. Different methods used: Assumptions and variables

Method	Assumptions	Variables (Gaussian model)	References
1	One phase representing the reaction product	Peak position / FWHH/ Intensity	
2	Two distinct phases are formed Phase 1 Phase 2	Peak position / FWHH / Intensity	
2-bis	Two distinct phases are formed		[22], [30], [46], [20]
	Phase 1	Peak position / FWHH/ Intensity	
	Phase 2 : Geopolymer GP	Intensity (Peak position and FWHH are maintained constant as plain metakaolin mixture)	
3	Deconvolution of reaction products using the minimum possible number of component peaks to represent mainly a 3D network structure	Intensity (Peak position : fixed from literature FWHH : constant for all the deconvoluted spectrum and <7ppm)	[27]

The first method, which is the simplest one, consists of the decomposition of the overall spectrum into three signals: remnant metakaolin, remnant slag (in binary mixtures), and a Gaussian signal representing the formed phase as presented in Figure 5. This deconvolution was conducted on all the mixtures. The results are given in Table 4. The formed phase in metakaolin system is centered between -90.9 ppm and -91.3 ppm at different ages. It shows that the shift in the overall ^{29}Si spectra (1 ppm to 2 ppm) is only an apparent shift as it results from the higher contribution of unreacted metakaolin overlapping with the peak of the

geopolymer formed which remains at the same position whatever the water content. This implies that water does not change the structure of the reaction product, i.e. a geopolymer structure is formed whatever H_2O/Na_2O ratios. A more notable difference in binary mixtures in the position of the reaction product can be observed by varying H_2O/Na_2O ratio. In the binary mixtures, the product shifts to higher frequencies compared to the geopolymer phase in activated metakaolin. Increasing water content leads to a lower dissolution of precursors due to its diluting effect and therefore a lower fraction of the binding phase. A high amount of unreacted metakaolin and slag, if any, can be detected at a high H_2O/Na_2O ratio. An increase in H_2O/Na_2O ratio results in a lower available OH^- concentration and limited dissolution of precursor, thus less aluminate and silicate monomers can participate in polymerization. Moreover, the dissolution of the aluminosilicate source and the ionization process consume hydroxides. Thus, the availability of hydroxides continuously decreases.

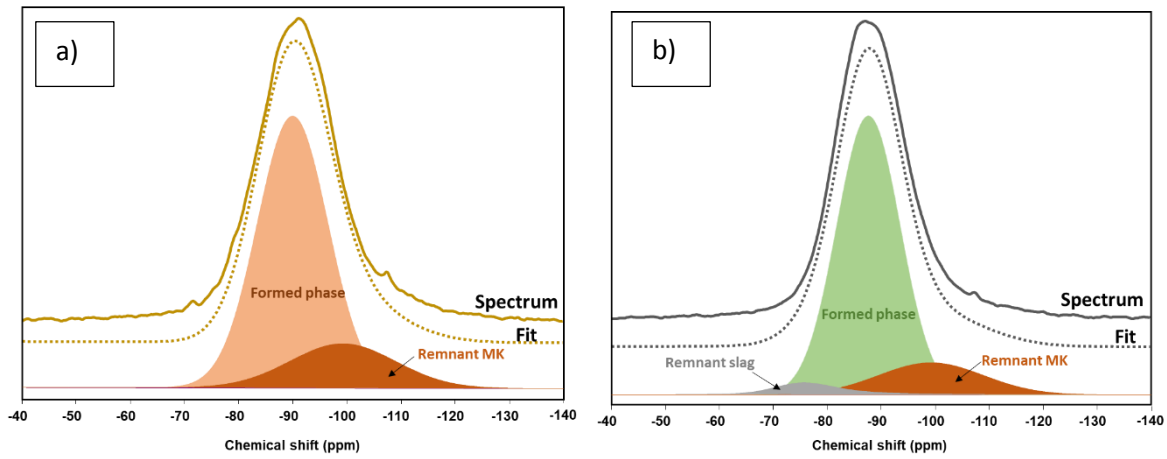

Figure 5. Decompositions of the ^{29}Si MAS NMR spectra of a) activated metakaolin MK21 and b) activated metakolin-slag MKS21 at 28 days using *method 1*

Table 4. Analysis of ^{29}Si NMR spectra using method 1

Mixtures		Remnant Slag mol-%Si	Remnant Metakaolin mol-%Si	Product Position (ppm)	Product FWHH	Product mol-%Si
MK21	28 d	-	20	-90.9	15.6	80
	250 d	-	17	-90.6	15.1	83
MK34	28 d	-	45	-91.3	15.5	55
	250 d	-	37	-90.7	16.4	63
MKS21	28 d	5	15	-87.6	13.9	80
	250 d	0.4	14	-87.5	13.7	85
MKS34	28 d	12	21	-88.4	13.9	67
	250 d	9	19	-88.3	13.9	72

Method 2 is based on previous studies reporting the presence of two distinct phases N-A-S-H and C-A-S-H in a blended material [20] [30] [15] [29] [22]. Thus, two Gaussian lines associated with the two-formed phases were used to obtain the best fit of the overall spectrum (Figure 6). Table 5 summarizes the obtained results. Phase 2 is in the region of Q^4(mAl) sites which defines a geopolymer structure whereas Phase 1 falls into the range of C-(A)-S-H gel at higher frequencies. The formation of Phase 1 is favored at a lower H_2O/Na_2O ratio with a preponderance of Phase 2 whatever the ages and the water content. By comparing Phase 2 to the formed phase in activated metakaolin material, there is a slight change in the position and the full width at half height decreases to 12. This suggests that the geopolymer structure has been modified by the incorporation of slag or that the method used does not allow assessing the real phase composition. Method 2 was modified (method 2-bis) by keeping the decomposition of the binding phase into two signals but here the phase 2, which represents the geopolymer, was directly extracted from the phase formed in the corresponding plain metakaolin mixture (MK21 at 28 days) at the same age and water content. The position and the width of phase 2 in MKS21 was fixed to -90.9 ppm and 15.6 respectively deduced from MK21 at 28 days (Table 4). Figure 7 shows the spectral deconvolution.

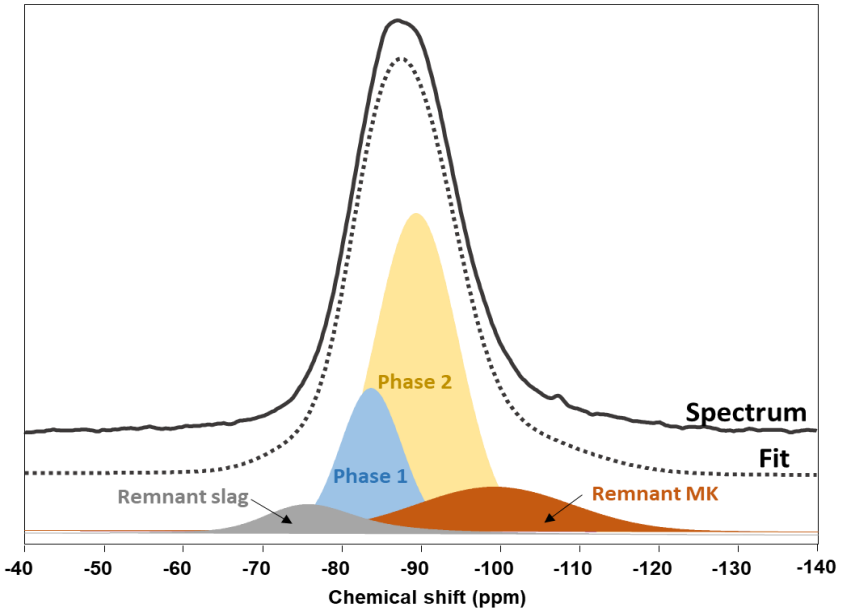

Figure 6. Decomposition of the ^{29}Si MAS NMR spectrum of activated metakolin-slag MKS21 at 28 days using *method 2*

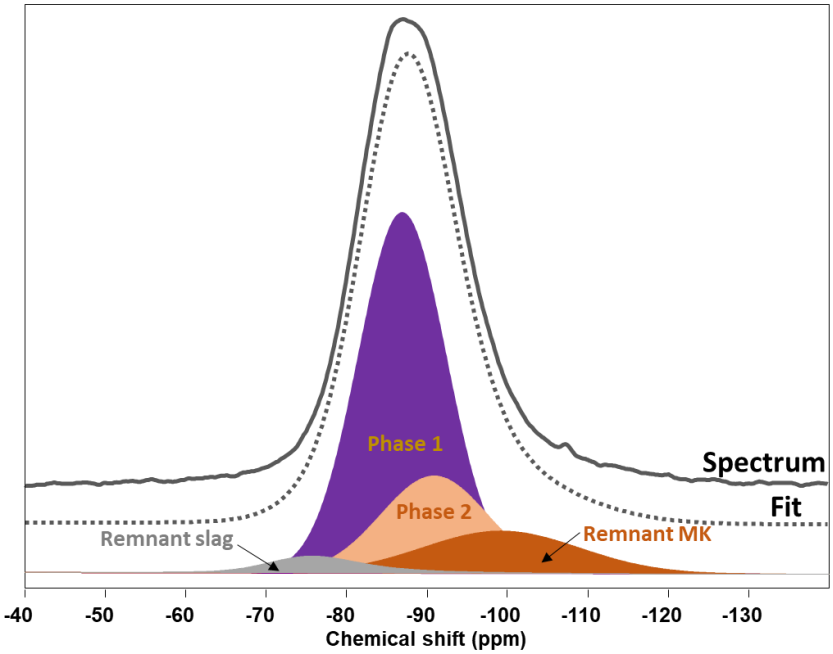

Figure 7. Decompositions of the ^{29}Si MAS NMR spectrum of activated metakolin-slag MKS21 at 28 days using *method 2-Bis*

The contribution of the geopolymer signal (phase 2) in the overall spectrum is surprisingly low compared to phase 1. Phase 1 is centered at -87 ppm and lies in the range of Q^1 to Q^4 sites. These results are in accordance with results obtained in a recent study on activated metakaolin containing calcium [26] [38]. It was suggested that a calcium-modified geopolymer (Ca,Na)-S-H with a three-dimensional structure was formed and presented a

Si/Al ratio lower than the conventional C-A-S-H gel with chain structures [38]. However, they reported that the 3D modified structure could not be presented directly from peak positions in the spectrum because the Q^4 peaks associated with three-dimensional structures would overlap with the sites on low frequencies associated with chain structures [38].

Table 5. Analysis of ^{29}Si NMR spectra using method 2 for binary mixtures

Mixtures		Remnant Slag mol-%Si	Remnant Metakaolin mol-%Si	Phase 1			Phase 2		
				Position (ppm)	FWHH	mol-%Si	Position (ppm)	FWHH	mol-%Si
MKS21	28 d	8	15	-83.7	9.0	19	-89.4	12.3	58
	250 d	6	14	-84.4	9.4	29	-90.0	12.1	51
MKS34	28 d	15	23	-82.9	8.0	4	-88.5	12.8	58
	250 d	12	18	-83.6	9.0	10	-89.4	12.9	60

Method 3 associates a Gaussian signal with each Q^4(mAl) site following Engelhard's notation [49]. Gaussian line model was used for deconvolution of ^{29}Si MAS NMR spectra using the minimum possible number of component peaks to describe accurately the spectrum. The full width at half-height (FWHH) and peak positions were kept constant throughout all spectral deconvolutions whenever possible. Peak locations were defined based on the available literature [20] [27] [50] [46]. Finally, the area of each component in ^{29}Si MAS NMR spectra represents the relative concentration of each Si species. ^{29}Si spectrum of binary mixtures is deconvoluted based on the study of Peres Cortes et al. [27] wherein an intermixed gel of sodium aluminosilicate hydrate (N-A-S-H) and sodium (calcium) aluminosilicate hydrate N-(C)–A-S-H with 3D network structures are formed in an alkali-activated metakaolin limestone cement. The resonances at -84.9, -89.7, -93.8, -98.3, and -103 ppm were attributed to Q^4 SiO_4 species coordinated with 4, 3, 2, 1, and 0 AlO_4 tetrahedral, respectively. The resonance at -78.1 and -79.9 ppm were associated with Q^1 and Q^2(1Al) species respectively. The peak at -

84.9 ppm that can overlap with Q^2 and Q^3(1Al) signals is assigned to Q^4(4Al) considering the significant intensity for AlO_4 species at 54-57 ppm observed by ^{27}Al MAS NMR [27].

Figure 8 shows that the peaks used to fit the ^{29}Si NMR spectra of the binary mixtures. The quantification of the different Q^n(mAl) species of binary mixtures is shown in Table 6. The equation for calculating the Si/Al molar ratio from Engelhard's formula [49] (Equation **(1)**) is used to determine the Si/Al ratio of the binding phase:

$$\frac{Si}{Al} = \frac{\sum_{n=0}^{4} Q^4(nAl)}{\sum_{n=0}^{4} \frac{n}{4} Q^4(nAl)} \qquad (1)$$

As a result, the amount of Q^2 species is relatively low compared to Q^4 species. The peak associated with Al-rich structural units Q^4(4Al) and Q^4(3Al) presented higher intensities at the expense of the Si-rich structural unit peaks. Thereby, a predominance of Al-rich structural units in the reaction products can be concluded. It is noteworthy to mention that this conclusion is always right by considering the hypothesis and the peak shifts attributed for each Si environment of method 3 as described above. However, a change of the signal attribution at -84.9 ppm for Q^2 and Q^3(1Al) signals would be enough to change the retained conclusions. In addition, a fit with a single component Q^2(1Al) is not representative of the gel 'C-A-S-H'. If there were only Q^2(1Al), the Si/Al ratio would be equal to 1 which is under the lower boundary of the conventional C-A-S-H [51] , there are necessarily Q^1,Q^2, and Q^3(1Al). In other words, some issues related to the deconvolution method imply remaining cautious about the results.

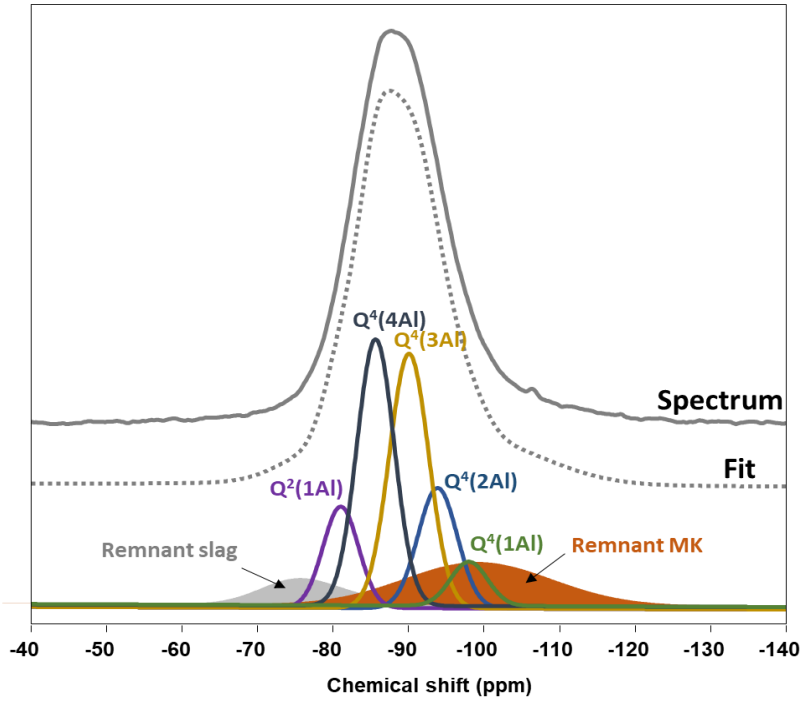

Figure 8. Decompositions of the ^{29}Si MAS NMR spectrum of activated metakaolin-slag MKS21 at 28 days using method 3

The Si/Al ratio of all mixtures lies between 1.28 and 1.33 (Table 6). These values are lower than that of the initial composition mixtures indicating preferential precipitation of an Al-rich gel. Increasing H_2O/Na_2O ratio resulted in a slight increase in Si/Al for the different formulations. Compared to the mixtures with a lower H_2O/Na_2O ratio, mixtures with a high H_2O/Na_2O ratio had higher remnant metakaolin, slag, and thus a lower percentage of reaction products. The amount of AlO_4 coordinated to SiO_4 was thus reduced due to a lower dissolution of precursors leading to a lower Al uptake in the binding phase. On the other hand, the trend of the variation of Si/Al in function of time is not clear. It is difficult to conclude on significant differences and evolutions. A small change of the signal attribution could modify the value of Si/Al. This underlines once again the issues related to the deconvolution method.

Table 6. Analysis of ^{29}Si NMR spectra using method 3 for binary mixtures

Position Gi (ppm) / mol-%Si		Remnant Slag	Remnant Metakaolin	Q^1 -78.14	$Q^2(1Al)$ -79.9	$Q^4(4Al)$ -84.9	$Q^4(3Al)$ -89.7	$Q^4(2Al)$ -93.8	$Q^4(1Al)$ -98.3	$Q^4(0Al)$ -103.6	Si/Al
MKS21	**28 d**	8	15	0	9	27	25	12	4	0	1.29
	250 d	5	14	0	9	29	27	12	4	0	1.28
MKS34	**28 d**	14	22	0	7	21	23	9	4	0	1.29
	250 d	12	19	0	7	22	24	12	4	0	1.33

The overall degree of reaction (RD_{ov}) can be determined from the amount of each phase formed in terms of Si mol%. It can be computed as Si mol% in the product with respect to that in the entire sample corresponding to product phase and unreacted metakaolin and slag (Equation **(2)**). The reaction degree is therefore equivalent to the amount of product.

$$RD_{ov}(Si) = \frac{\boldsymbol{Moles\ of\ Si\ in\ product\ phase}}{\boldsymbol{Moles\ of\ total\ Si\ in\ sample}} \qquad \textbf{(2)}$$

The reaction degree of metakaolin RD_{mk} (Equation (**3**)) and slag RD_s (Equation (**4**)) can be calculated separately. $\boldsymbol{X(Si)_{mk}}$ and $\boldsymbol{X(Si)_s}$ refer to the silicon provided by metakaolin and slag respectively and determined from their chemical composition (Table 1). Only the amorphous fraction of the metakaolin is considered in the calculation.

$$RD_{mk} = \frac{\boldsymbol{X(Si)_{mk} - R_{mk}}}{\boldsymbol{X(Si)_{mk}}} \qquad \textbf{(3)}$$

$$RD_s = \frac{\boldsymbol{X(Si)_s - R_s}}{\boldsymbol{X(Si)_s}} \qquad \textbf{(4)}$$

The results are given in Table 7. It can be concluded that the decomposition methods mostly agree with each other in terms of reaction degree. Nevertheless, the challenge lies in the representation of the products. In Figure 9, an average value and the difference between the three methods are represented with a difference between the minimum and the maximum values.

Table 7 Reaction degrees provided by the different methods

Mixtures	Days	Method 1			Method 2			Method 3		
		RD_{mk}	RD_s	RD_{ov}	RD_{mk}	RD_s	RD_{ov}	RD_{mk}	RD_s	RD_{ov}
MK21	**28**	63	-	80	-	-	-	-	-	-
	250	68	-	82	-	-	-	-	-	-
MK34	**28**	17	-	54	-	-	-	-	-	-
	250	32	-	63	-	-	-	-	-	-
MKS21	**28**	61	73	80	62	56	77	61	54	77
	250	64	98	85	65	67	80	65	70	82
MKS34	**28**	46	32	67	43	10	62	44	16	63
	250	53	47	72	54	32	70	51	29	69

Figure 9 shows the reaction degree of the different mixtures. MK21 and MKS21 present a higher reaction degree than high H_2O/Na_2O mixtures. Replacing a part of metakaolin by slag slightly changes the overall reaction degree but it influences differently the reactivity of metakaolin depending on the H_2O/Na_2O ratios. At low water content, the reactivity of metakaolin does not seem to be influenced by the addition of slag to the mixture. The overall reaction degree reached 80 % and the reaction degree of metakaolin was 63% and 61 % in MK21 and MKS21 at 28 days respectively. These values slightly increased after 250 days. A different trend can be noticed at a higher H_2O/Na_2O ratio. Replacing metakaolin by slag in MK34 increased the reactivity of metakaolin from 17% to 44 %. It would mean that slag enhanced the dissolution of metakaolin; however, the overall reaction remained low. This is consistent with previous study stating that adding calcium to the metakolin systems enhanced the dissolution of metakaolin and increased the reaction degree [38] [26] [20]. The formation of C-A-S-H at early age of reaction in a calcium-rich medium consumes silicate in the pore solution, which enhances the dissolution of metakaolin to sustain the silicate concentration leading to a release of aluminates [52] [53]. Besides, the formation of C-A-S-H also consumes water, which increases the alkalinity of the system and further enhances the dissolution of precursor [53]. As calcium reduces silicate in solution, the protective layer of aluminosilicate

gel, which forms on metakaolin surface mainly in the silicate-activated mixes [54], is less likely to form and limit further dissolution.

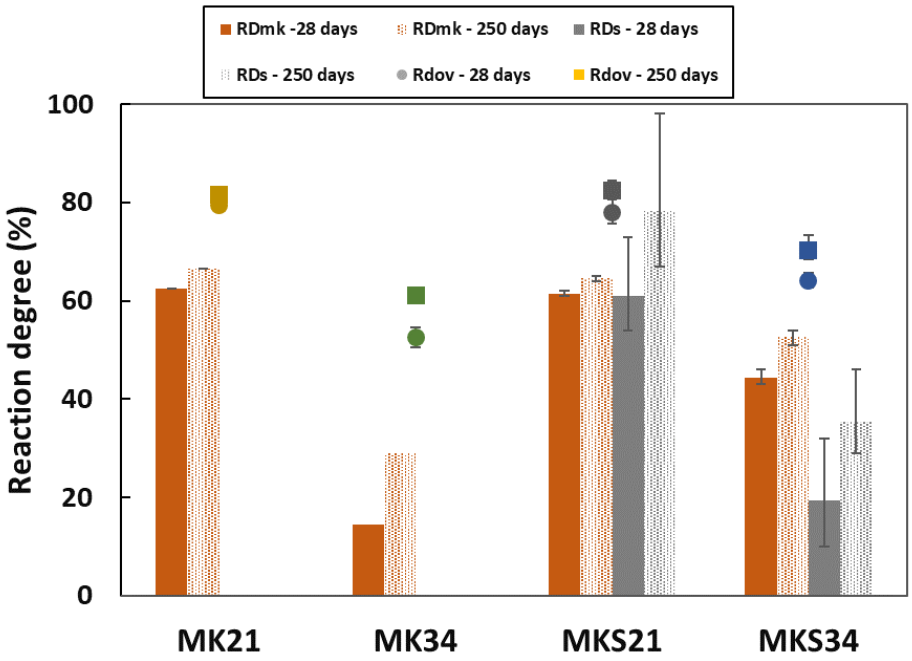

Figure 9. Comparison of reaction degree, calculation from ^{29}Si NMR spectroscopy; the error bars represents the difference between the methods used

Finally, compressive strength at 28 days is plotted versus the reaction degree Si mol% (RD_{ov} , RD_{mk}, RD_s) (see Figure 10). It was reported that compressive strength is linearly correlated with the reaction degree [38]. However, the compressive strength in our study does not seem to be linearly correlated with the degree of reaction. MK21 and MKS21 exhibited similar reaction degrees (RD_{ov} , RD_{mk}) whereas they developed different compressive strengths. The strength does not only depend on reaction degree but also on the proportion of solid phase and microstructural parameters. The solid phase content depends on initial proportion of solid reactants and chemically bound water. The combination of C-A-S-H and calcium-modified geopolymer gel produces strength more efficiently than mixtures containing only plain geopolymer gel. The positive effect of adding calcium on compressive strength was reported previously [23] [38] [27]. At high H_2O/Na_2O, the slight increase in compressive strength of

MKS34 compared to MK34 is due to both the increase in the reactivity of metakaolin and the presence of calcium in the mixture. However, both the reactivity of metakaolin and slag are influenced by high water content. This could suggest similar factors affecting the initial dissolution of precursors that prevent further dissolution at high water content and the mechanism of formation of the product phase.

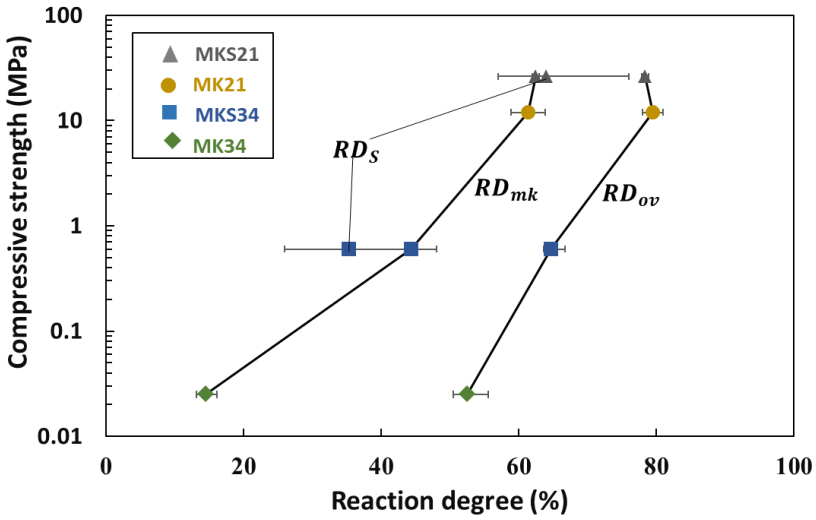

Figure 10. Compressive strength versus the degree of reaction at 28 days

4. General discussion

The studied materials cover a range of compositions and properties where H_2O/Na_2O varies from 21 to 34 and the slag proportion from 0 to 25% as a replacement of metakaolin. Increasing water content has been reported to induce changes in the kinetics of the process and the composition and nanostructure of the reaction products [29] [8] [9]. N-A-S-H precipitated with various types of zeolite related generally to low strength materials as reported in [35], however they were not detected in the present study through XRD. ^{27}Al and ^{29}Si MAS NMR spectroscopy, which provide further insight into the amorphous structure of the product phase, showed that the variation of H_2O/Na_2O ratio would not change the type of product formed in activated metakolin and binary mixtures. Therefore, the drop in compressive strength with higher H_2O/Na_2O can be attributed to the influence on the

reactivity of the precursor and the lower fraction of binding phase rather than the change of products composition or zeolite phase formation in the range of molar ratios studied in this work.

NMR results showed that the main reaction product in activated metakaolin system is the so-called geopolymer gel N-A-S-H regardless the H_2O/Na_2O ratio; its fraction increased with reaction time especially at high H_2O/Na_2O ratio. Regarding the product phase in binary mixtures, different methods have been exposed and implemented taking into account the different approaches found in the literature. ^{29}Si spectra of binary mixtures shifted to higher frequencies than plain metakaolin based material. Method 2 proves that the distinction of two phases attributed respectively to the conventional C-A-S-H (higher frequencies) and the 3D polymerized network (lower frequencies) does not represent the real phase composition. This is due to the modified phase formed at lower frequencies which does not represent the geopolymer structure obtained in a plain metakaolin mixture. Besides, method 2-bis confirmed the formation of a phase that lies between higher and lower frequencies. Chen et al. [26] [38] have attributed this phase to the contribution of both C-A-S-H phase with chain structures and calcium-modified geopolymer (Ca,Na)-A-S-H with a three-dimensional structure. Another study suggested the possibility for Q^2 and q^4 species to belong to the same phase in contradiction with the structure of both 3D network and C-A-S-H [55].

Method 3 concurred with the conclusion of method 2. It was based on the proposed peak positions in the ^{29}Si spectrum of an intermixed N-A-S-H and N-(C)-A-S-H both with 3D network structure [27]. At low pH value (<12), Ca-exchanged N-A-S-H appear to give (N, C)-A-S-H by ion exchange until all Na has been replaced by Ca which retain its 3D aluminosilicate framework. (N, C)-A-S-H exists at a pH<12 value and within the range of composition limits Na/Al<1.85 and Ca/Si<0.3 which is compatible with our initial composition (Na/Al=1 and Ca/Si =0.21) [17]. However, this method neglects the existence of

complex phases (presence of Q^2 and Q^3), which are not considered in the analysis. The peaks were chosen to define mainly a 3D structure with Q^4 Si species. In other words, we cannot exclude the possibility of the presence of Q^3 and Q^3(1Al) or the presence of a transitional phase between C-A-S-H and N-A-S-H expected to coexist in such systems, which implies the limit related to the deconvolution method.

Based on these interpretations, a conceptual model of the process can be proposed. The evolution of the polymerized network towards a well-defined C-A-S-H goes through the formation of a heterogeneous phase involved in the transformation of the 3D network to C-A-S-H. This heterogeneous phase can be supported by the presence of local structures at high and low frequencies, which are linked by q^4 Al species. The evolution of ^{29}Si spectra of the binary mixtures (Figure 11) especially the ^{29}Si spectra of the mixture MKS34 after a long time (after 500 days) confirms the suggested process model. The main resonance peak observed at 28 and 250 days on the ^{29}Si spectra widened after 500 days and a peak at -86 ppm started to appear as in the case of MKS21. This peak can be linked to the formation of Q^2 species in C-A-S-H. However, the ^{27}Al spectra do not show any remarkable evolution after 500 days compared to 28 and 250 days for the two mixtures MKS21 and MKS34 (Figure A. 1 in Appendix). Once again, these results shows that the same phase is formed in the two mixtures with a delayed evolution due to the effect of water. In addition, the evolution between ^{29}Si spectra of the mixture MKS21 at 250 days and after 500 days may suggest the possible stability of this phase.

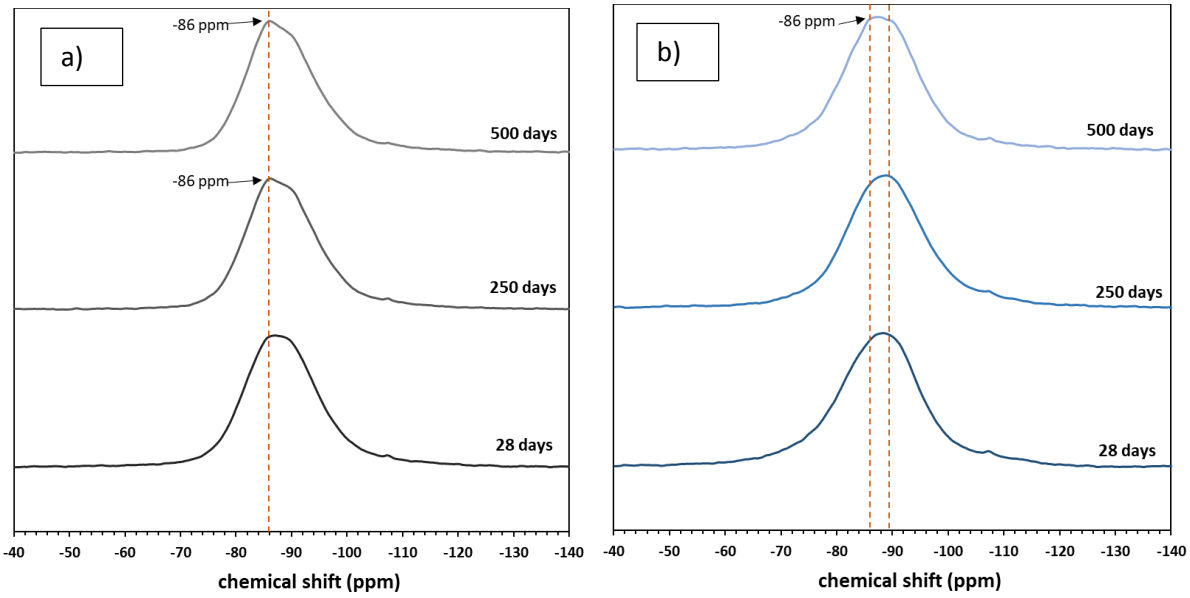

Figure 11. ^{29}Si MAS NMR spectra of activated metakaolin-slag systems (a) MKS21 (b) MKS34 at 28, 250, and 500 days

Finally, the evaluation of the reaction degree showed that adding slag to the mixture increased the reactivity of metakaolin and resulted in higher compressive strength in comparison to plain metakaolin mixtures. However, plain metakaolin and binary mixtures showed similar behavior about the drop in compressive strength at high H_2O/Na_2O.

5. Conclusion

In this article, different approaches, based on the different opinions evoked in the literature, were discussed to explore the phase composition in binary activated metakaolin mixtures with 25% of slag, by comparison with plain metakaolin mixtures. The influence of the incorporation of calcium on the local structure was investigated. The effect of H_2O/Na_2O ratio, which is a key parameter to design alkali-activated materials, was also studied. The following conclusions can be drawn from experimental results and their analysis:

- The challenge of the decomposition methods lied in the representation of the products, however they agreed with each other in term of reaction degree. A particular attention

should be paid to the use of the deconvolution method, as different peaks could be present at the same chemical shifts thus some will be neglected.

- The analysis of the phase composition of a mixture containing 25% of slag and 75 % of metakaolin as precursors suggested the presence of a heterogeneous phase involved in the transformation of 3D network to C-A-S-H , supporting the presence of local structures at high and low frequencies, which are linked by q^4 Al species. This suggestion is based on the comparison of different approaches.
- Increasing H_2O/Na_2O ratio in plain and binary mixtures resulted in higher content of unreacted precursors and a lower product fraction without changing the local structure of products, which can explain the drop in the compressive strength as H_2O/Na_2O increased.
- Adding slag to the mixture increased the reactivity of metakaolin and resulted in higher compressive strength in comparison with plain metakaolin mixtures.

Finally, it seems interesting to study the durability and the ion transport properties of these materials, which are partly controlled by gel nanostructure.

CRediT authorship contribution statement

F. Souayfan: Investigation, formal analysis, writing - original draft;
E. Rozière: Supervision, formal analysis, writing - review & editing;
M. Paris: Investigation, formal analysis, writing – review & editing;
D. Deneele: Investigation, formal analysis,
A. Loukili: Funding acquisition, supervision,
C. Justino: Funding acquisition, supervision

Acknowledgements

Funding: The authors would like to acknowledge financial and technical support of Soletanche Bachy France.

Declaration of Competing Interest

The authors declare that they have no known competing financial interests or personal relationships that could have appeared to influence the work reported in this paper.

References

[1] H. Güllü et A. Ali Agha, « The rheological, fresh and strength effects of cold-bonded geopolymer made with metakaolin and slag for grouting », *Construction and Building Materials*, vol. 274, p. 122091, mars 2021, doi: 10.1016/j.conbuildmat.2020.122091.

[2] H. Güllü, M. M. D. Al Nuaimi, et A. Aytek, « Rheological and strength performances of cold-bonded geopolymer made from limestone dust and bottom ash for grouting and deep mixing », *Bull Eng Geol Environ*, oct. 2020, doi: 10.1007/s10064-020-01998-2.

[3] A. Hassan, M. Arif, et M. Shariq, « Use of geopolymer concrete for a cleaner and sustainable environment – A review of mechanical properties and microstructure », *Journal of Cleaner Production*, vol. 223, p. 704‑728, juin 2019, doi: 10.1016/j.jclepro.2019.03.051.

[4] Y. Wu, B. Lu, Z. Yi, F. Du, et Y. Zhang, « The Properties and Latest Application of Geopolymers », *IOP Conf. Ser.: Mater. Sci. Eng.*, vol. 472, p. 012029, févr. 2019, doi: 10.1088/1757-899X/472/1/012029.

[5] J. L. Provis, « Geopolymers and other alkali activated materials: why, how, and what? », *Mater Struct*, p. 15, 2014, doi: 10.1617/s11527-013-0211-5.

[6] R. J. Myers, S. A. Bernal, R. San Nicolas, et J. L. Provis, « Generalized Structural Description of Calcium–Sodium Aluminosilicate Hydrate Gels: The Cross-Linked Substituted Tobermorite Model », *Langmuir*, vol. 29, n° 17, p. 5294‑5306, 2013, doi: 10.1021/la4000473.

[7] I. G. Richardson, « The calcium silicate hydrates », *Cement and Concrete Research*, vol. 38, n° 2, p. 137‑158, févr. 2008, doi: 10.1016/j.cemconres.2007.11.005.

[8] K. Scrivener, F. Martirena, S. Bishnoi, et S. Maity, « Calcined clay limestone cements (LC3) », *Cement and Concrete Research*, vol. 114, p. 49‑56, déc. 2018, doi: 10.1016/j.cemconres.2017.08.017.

[9] A. Fernandez-Jimenez, I. García-Lodeiro, et A. Palomo, « Durability of alkali-activated fly ash cementitious materials », *J Mater Sci*, vol. 42, n° 9, p. 3055‑3065, mai 2007, doi: 10.1007/s10853-006-0584-8.

[10] R. Pouhet et M. Cyr, « Studies of Natural and Accelerated Carbonation in Metakaolin-Based Geopolymer », *AST*, vol. 92, p. 38‑43, oct. 2014, doi: 10.4028/www.scientific.net/AST.92.38.

[11] M. Zhang, M. Zhao, G. Zhang, P. Nowak, A. Coen, et M. Tao, « Calcium-free geopolymer as a stabilizer for sulfate-rich soils », *Applied Clay Science*, vol. 108, p. 199‑207, mai 2015, doi: 10.1016/j.clay.2015.02.029.

[12] S. Rios, C. Ramos, A. Viana da Fonseca, N. Cruz, et C. Rodrigues, « Mechanical and durability properties of a soil stabilised with an alkali-activated cement », *European Journal of Environmental and Civil Engineering*, vol. 23, n° 2, p. 245‑267, févr. 2019, doi: 10.1080/19648189.2016.1275987.

[13] N. B. Singh et B. Middendorf, « Geopolymers as an alternative to Portland cement: An overview », *Construction and Building Materials*, vol. 237, p. 117455, mars 2020, doi: 10.1016/j.conbuildmat.2019.117455.
[14] L. K. Turner et F. G. Collins, « Carbon dioxide equivalent (CO2-e) emissions: A comparison between geopolymer and OPC cement concrete », *Construction and Building Materials*, vol. 43, p. 125‑130, juin 2013, doi: 10.1016/j.conbuildmat.2013.01.023.
[15] *Handbook of Alkali-Activated Cements, Mortars and Concretes*. Elsevier, 2015. doi: 10.1016/C2013-0-16511-7.
[16] A. Cherki El Idrissi, M. Paris, E. Rozière, D. Deneele, S. Darson, et A. Loukili, « Alkali-activated grouts with incorporated fly ash: From NMR analysis to mechanical properties », *Materials Today Communications*, vol. 14, p. 225‑232, mars 2018, doi: 10.1016/j.mtcomm.2018.01.012.
[17] I. Garcia-Lodeiro, A. Palomo, A. Fernández-Jiménez, et D. E. Macphee, « Compatibility studies between N-A-S-H and C-A-S-H gels. Study in the ternary diagram Na2O–CaO–Al2O3–SiO2–H2O », *Cement and Concrete Research*, vol. 41, n° 9, p. 923‑931, sept. 2011, doi: 10.1016/j.cemconres.2011.05.006.
[18] S. A. Bernal, J. L. Provis, V. Rose, et R. Mejía de Gutierrez, « Evolution of binder structure in sodium silicate-activated slag-metakaolin blends », *Cement and Concrete Composites*, vol. 33, n° 1, p. 46‑54, janv. 2011, doi: 10.1016/j.cemconcomp.2010.09.004.
[19] S. A. Bernal, E. D. Rodríguez, R. Mejía de Gutiérrez, M. Gordillo, et J. L. Provis, « Mechanical and thermal characterisation of geopolymers based on silicate-activated metakaolin/slag blends », *J Mater Sci*, vol. 46, n° 16, p. 5477‑5486, août 2011, doi: 10.1007/s10853-011-5490-z.
[20] A. Buchwald, H. Hilbig, et Ch. Kaps, « Alkali-activated metakaolin-slag blends—performance and structure in dependence of their composition », *J Mater Sci*, vol. 42, n° 9, p. 3024‑3032, mai 2007, doi: 10.1007/s10853-006-0525-6.
[21] S. A. Bernal, « Effect of the activator dose on the compressive strength and accelerated carbonation resistance of alkali silicate-activated slag/metakaolin blended materials », *Construction and Building Materials*, vol. 98, p. 217‑226, nov. 2015, doi: 10.1016/j.conbuildmat.2015.08.013.
[22] O. Burciaga-Díaz, R. X. Magallanes-Rivera, et J. I. Escalante-García, « Alkali-activated slag-metakaolin pastes: strength, structural, and microstructural characterization », *Journal of Sustainable Cement-Based Materials*, p. 18, 2013, doi: 10.1080/21650373.2013.801799.
[23] O. Burciaga-Díaz, J. I. Escalante-García, R. Arellano-Aguilar, et A. Gorokhovsky, « Statistical Analysis of Strength Development as a Function of Various Parameters on Activated Metakaolin/Slag Cements », *Journal of the American Ceramic Society*, vol. 93, n° 2, p. 541‑547, févr. 2010, doi: 10.1111/j.1551-2916.2009.03414.x.
[24] G. Samson, M. Cyr, et X. X. Gao, « Formulation and characterization of blended alkali-activated materials based on flash-calcined metakaolin, fly ash and GGBS », *Construction and Building Materials*, vol. 144, p. 50‑64, juill. 2017, doi: 10.1016/j.conbuildmat.2017.03.160.
[25] A. Hasnaoui, E. Ghorbel, et G. Wardeh, « Optimization approach of granulated blast furnace slag and metakaolin based geopolymer mortars », *Construction and Building Materials*, vol. 198, p. 10‑26, févr. 2019, doi: 10.1016/j.conbuildmat.2018.11.251.
[26] X. Chen, A. Sutrisno, et L. J. Struble, « Effects of calcium on setting mechanism of metakaolin-based geopolymer », *Journal of the American Ceramic Society*, p. 12, 2017, doi: 10.1111/jace.15249.
[27] P. Perez-Cortes et J. I. Escalante-Garcia, « Gel composition and molecular structure of alkali-activated metakaolin-limestone cements », *Cement and Concrete Research*, p. 13, 2020, doi: 10.1016/j.cemconres.2020.106211.
[28] B. Walkley et J. L. Provis, « Solid-state nuclear magnetic resonance spectroscopy of cements », *Materials Today Advances*, vol. 1, p. 100007, mars 2019, doi: 10.1016/j.mtadv.2019.100007.
[29] C. Ruiz-Santaquiteria, J. Skibsted, A. Fernández-Jiménez, et A. Palomo, « Alkaline solution/binder ratio as a determining factor in the alkaline activation of aluminosilicates », *Cement and Concrete Research*, p. 10, 2012, doi: 10.1016/j.cemconres.2012.05.019.

[30] A. Aboulayt *et al.*, « Alkali-activated grouts based on slag-fly ash mixtures: From early-age characterization to long-term phase composition », *Construction and Building Materials*, vol. 260, p. 120510, nov. 2020, doi: 10.1016/j.conbuildmat.2020.120510.

[31] F. Cassagnabère, P. Diederich, M. Mouret, G. Escadeillas, et M. Lachemi, « Impact of metakaolin characteristics on the rheological properties of mortar in the fresh state », *Cement and Concrete Composites*, vol. 37, p. 95‑107, mars 2013, doi: 10.1016/j.cemconcomp.2012.12.001.

[32] P. Duxson, A. Fernández-Jiménez, J. L. Provis, G. C. Lukey, A. Palomo, et J. S. J. van Deventer, « Geopolymer technology: the current state of the art », *J Mater Sci*, vol. 42, nº 9, p. 2917‑2933, mai 2007, doi: 10.1007/s10853-006-0637-z.

[33] A. Cherki El Idrissi, « The development of a global mix design and analysis approach for alkali activated soil reinforcement grouts », *European Journal of Environmental and Civil Engineering*, vol. 23, nº 5, p. 645‑656, mai 2019, doi: 10.1080/19648189.2018.1519461.

[34] M. Lizcano, A. Gonzalez, S. Basu, K. Lozano, et M. Radovic, « Effects of Water Content and Chemical Composition on Structural Properties of Alkaline Activated Metakaolin-Based Geopolymers », *J. Am. Ceram. Soc.*, vol. 95, nº 7, p. 2169‑2177, juill. 2012, doi: 10.1111/j.1551-2916.2012.05184.x.

[35] V. Benavent, F. Frizon, et A. Poulesquen, « Effect of composition and aging on the porous structure of metakaolin-based geopolymers », *J Appl Crystallogr*, vol. 49, nº 6, p. 2116‑2128, déc. 2016, doi: 10.1107/S1600576716014618.

[36] K. Juengsuwattananon, F. Winnefeld, P. Chindaprasirt, et K. Pimraksa, « Correlation between initial SiO2/Al2O3, Na2O/Al2O3, Na2O/SiO2 and H2O/Na2O ratios on phase and microstructure of reaction products of metakaolin-rice husk ash geopolymer », *Construction and Building Materials*, vol. 226, p. 406‑417, nov. 2019, doi: 10.1016/j.conbuildmat.2019.07.146.

[37] K. Juengsuwattananon et K. Pimraksa, « VARIABLE FACTORS CONTROLLING AMORPHOUS-ZEOLITE PHASE TRANSFORMATION IN METAKAOLIN BASED GEOPOLYMER », *Acta Metall Slovaca*, vol. 23, nº 4, p. 378‑386, déc. 2017, doi: 10.12776/ams.v23i4.1001.

[38] X. Chen, E. Kim, P. Suraneni, et L. Struble, « Quantitative Correlation between the Degree of Reaction and Compressive Strength of Metakaolin-Based Geopolymers », *Materials*, vol. 13, nº 24, p. 5784, déc. 2020, doi: 10.3390/ma13245784.

[39] Z. Sun et A. Vollpracht, « Isothermal calorimetry and in-situ XRD study of the NaOH activated fly ash, metakaolin and slag », *Cement and Concrete Research*, vol. 103, p. 110‑122, janv. 2018, doi: 10.1016/j.cemconres.2017.10.004.

[40] B. Walkley *et al.*, « Phase evolution of C-(N)-A-S-H/N-A-S-H gel blends investigated via alkali-activation of synthetic calcium aluminosilicate precursors », *Cement and Concrete Research*, vol. 89, p. 120‑135, nov. 2016, doi: 10.1016/j.cemconres.2016.08.010.

[41] I. Sobrados et J. Sanz, « A´ ngel Palomo, Santiago Alonso, and Ana Fernandez-Jime´nez », *Journal of the American Ceramic Society*, vol. 87, nº 6, p. 5, 2004.

[42] J. Davidovits, « GEOPOLYMERS: Man-Made Rock Geosynthesis and the Resulting Development of Very Early High Strength Cement », p. 25.

[43] C. Li, H. Sun, et L. Li, « A review: The comparison between alkali-activated slag (Si+Ca) and metakaolin (Si+Al) cements », *Cement and Concrete Research*, vol. 40, nº 9, p. 1341‑1349, sept. 2010, doi: 10.1016/j.cemconres.2010.03.020.

[44] B. Walkley, X. Ke, O. H. Hussein, S. A. Bernal, et J. L. Provis, « Incorporation of strontium and calcium in geopolymer gels », *Journal of Hazardous Materials*, vol. 382, p. 121015, janv. 2020, doi: 10.1016/j.jhazmat.2019.121015.

[45] I. Garcı´a-Lodeiro, A. Ferna´ndez-Jime´nez, A. Palomo, et D. E. Macpheey, « Effect of Calcium Additions on NASH Cementitious Gels », *Journal of the American Ceramic Society*, vol. 93, nº 7, p. 7, 2010, doi: 10.1111/j.1551-2916.2010.03668.x.

[46] S. A. Bernal *et al.*, « Gel nanostructure in alkali-activated binders based on slag and fly ash, and effects of accelerated carbonation », *Cement and Concrete Research*, vol. 53, p. 127‑144, nov. 2013, doi: 10.1016/j.cemconres.2013.06.007.

[47] D. Massiot *et al.*, « Modelling one- and two-dimensional solid-state NMR spectra: Modelling 1D and 2D solid-state NMR spectra », *Magn. Reson. Chem.*, vol. 40, n° 1, p. 70‑76, janv. 2002, doi: 10.1002/mrc.984.
[48] S. Puligilla et P. Mondal, « Co-existence of aluminosilicate and calcium silicate gel characterized through selective dissolution and FTIR spectral subtraction », *Cement and Concrete Research*, p. 11, 2015, doi: 10.1016/j.cemconres.2015.01.006.
[49] G. Engelhardt, « Multinuclear solid-state NMR in silicate and zeolite chemistry », *TrAC Trends in Analytical Chemistry*, vol. 8, n° 9, p. 343‑347, oct. 1989, doi: 10.1016/0165-9936(89)87043-8.
[50] A. Buchwald, « Condensation of aluminosilicate gels—model system for geopolymer binders », *Journal of Non-Crystalline Solids*, p. 7, 2011, doi: https://doi.org/10.1016/j.jnoncrysol.2010.12.036.
[51] R. J. Myers, E. L'Hôpital, J. L. Provis, et B. Lothenbach, « Effect of temperature and aluminium on calcium (alumino)silicate hydrate chemistry under equilibrium conditions », *Cement and Concrete Research*, vol. 68, p. 83‑93, févr. 2015, doi: 10.1016/j.cemconres.2014.10.015.
[52] S. Puligilla et P. Mondal, « Role of slag in microstructural development and hardening of fly ash-slag geopolymer », *Cement and Concrete Research*, vol. 43, p. 70‑80, janv. 2013, doi: 10.1016/j.cemconres.2012.10.004.
[53] J. Temuujin, A. van Riessen, et R. Williams, « Influence of calcium compounds on the mechanical properties of fly ash geopolymer pastes », *Journal of Hazardous Materials*, vol. 167, n° 1‑3, p. 82‑88, août 2009, doi: 10.1016/j.jhazmat.2008.12.121.
[54] X. Chen, A. Sutrisno, L. Zhu, et L. J. Struble, « Setting and nanostructural evolution of metakaolin geopolymer », *J Am Ceram Soc*, vol. 100, n° 5, p. 2285‑2295, mai 2017, doi: 10.1111/jace.14641.
[55] E. Coudert, M. Paris, D. Deneele, G. Russo, et A. Tarantino, « Use of alkali activated high-calcium fly ash binder for kaolin clay soil stabilisation: Physicochemical evolution », *Construction and Building Materials*, vol. 201, p. 539‑552, mars 2019, doi: 10.1016/j.conbuildmat.2018.12.188.

Appendix

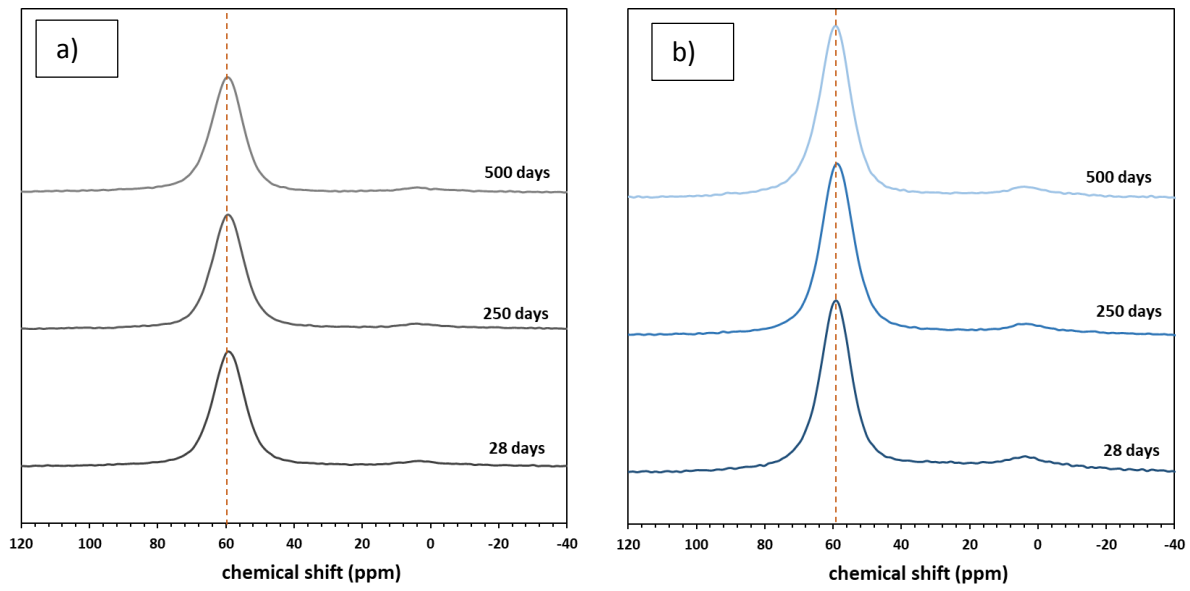

Figure A. 1 ^{27}Al MAS NMR spectra of activated metakaolin-slag systems (a) MKS21 (b) MKS34 at 28, 250, and 500 days

^{29}Si and ^{27}Al MAS NMR spectroscopic studies of activated metakaolin-slag mixtures

Faten Souayfan[a], Emmanuel Rozière[a], Michaël Paris[b], Dimitri Deneele[b,c], Ahmed Loukili[a], Christophe Justino [d]

[a] Civil engineering and Mechanics Research Institute (GeM), UMR-CNRS 6183, Ecole Centrale de Nantes, 1 rue de la Noe – 44321 Nantes, France

[b] Université de Nantes, CNRS, Institut des Matériaux Jean Rouxel, IMN, F-44000 Nantes, France

[c] GERS-LGIE, Université Gustave Eiffel, IFSTTAR, F-44344 Bouguenais, France

[d] Soletanche-Bachy, Chemin des Processions – 77130 Montereau Fault Yonne, France

Abstract

Blending metakaolin with slag in alkali-activated materials represents a promising way to achieve both acceptable engineering properties and durability. Nuclear Magnetic Resonance (NMR) spectroscopy has appeared as a key technique to investigate the structure of alkali-activation products. However, there is not a consensus on the analysis of NMR spectra to identify the phases formed in binary slag-metakaolin mixtures. This paper characterizes the phase composition and the reaction degree of alkali-activated metakaolin-slag blends, with special emphasis on the effect of H_2O/Na_2O ratio. Different approaches based on the literature are presented and implemented to analyze NMR data. The results suggest the formation of a heterogeneous phase involved in the transformation of 3D network to C-A-S-H. The evaluation of the reaction degree showed that the incorporation of slag in activated metakaolin mixtures resulted in higher reactivity of metakaolin and higher compressive strength.

Keywords

Alkali activated materials, Metakaolin, Slag, Sodium silicate Reaction degree, ^{29}Si MAS NMR, ^{27}Al MAS NMR, Geopolymer, Strength

1. Introduction

Alkali-activated materials (AAM) are considered as a next-generation material to replace Portland cement-based materials for durability purposes in some severe conditions [1]–[4]. They can be obtained by the activation of solid aluminosilicate sources at high pH [5]. Metakaolin and ground granulated blast furnace slag (GGBFS) are the most frequently used materials in AAM production. Ground granulated blast furnace slag (GGBFS) is widely used due to its composition and relatively low cost as an industrial by-product. The main reaction product of the activation of slag is calcium silicate hydrates substituted with aluminum (C-A-S-H) favored by its high calcium content [6], [7]. On the other hand, metakaolin is obtained by the calcination of kaolinitic clays which are considered available enough to meet the demand for building materials [8]. Metakaolin was found more suitable to be used for alkali-activation due to better durability [9]–[13] and possibly lower carbon footprint [14]. Its alkaline activation results in the formation of a geopolymer structure (N-A-S-H) [15]–[17] instead of hydration products with chemically bound water. The development of AAM using blended binders of metakaolin and slag is promising to compensate for the limitation related to each type of precursors. Hybrid metakaolin-slag material has been studied for the last decade [18]–[24]. These binders usually present improved properties compared to systems where metakaolin or slag are activated alone. Only 2% of investigations in recent studies on geopolymer-based materials have focused on binary metakaolin and slag mixtures as reported in [25]. The studies were mainly carried out on concretes and mortars. However, the phase composition was the subject of only a few studies. It was reported that their microstructure includes co-existing Ca-rich and Na-rich reaction products [20], [22]. The presence of geopolymer and slag-based binder in different proportions depending on their composition in a metakaolin-slag material was stated [20] [26]. Other studies mentioned the coexistence of N-A-S-H and N-(C)-A-S-H, both with a 3D network structure, intermixed with C-A-S-H, in

alkali-activated metakaolin-limestone cement [27] [26]. However, there are dispersed opinions describing the phase composition of a hybrid system related to the variety of chemical compositions and amorphous fraction reactivity of the precursors.

Nuclear magnetic resonance (NMR) has become a key tool to study AAM [28]. This method actually allows investigating the local chemical environments regardless of the level of disorder. ^{29}Si and ^{27}Al MAS NMR spectra are usually analyzed to explore the phase composition in alkali-activated materials. The spectral deconvolutions, using appropriate models and constraints, have been used to quantify the reaction products and to calculate the reaction degree [20], [27], [29], [30]. However, the overlap of potential peaks induces ambiguity in their attribution. This puts into question the peak deconvolution methods used in previous works.

The present study aims at investigating the phase composition in binary mixtures using ^{29}Si and ^{27}Al MAS NMR spectra. Different approaches, using ^{29}Si spectra, will be discussed taking into account the different opinions evoked in the literature concerning the present phases and the deconvolution methods. A comparison of different approaches and assumptions, implemented on the same NMR spectra, cannot be found in the literature.

Therefore, the main purpose of this study is to understand the phase composition in binary mixtures by dissecting the different opinions and approaches using ^{27}Al and ^{29}Si MAS NMR spectra. XRD (X-ray diffraction method) was also used to detect the apparition of crystallized phases, if any. A combination of slag and metakaolin at 25% and 75 % respectively has been selected to elaborate the studied materials and they were compared with plain metakaolin mixtures. The influence of H_2O/Na_2O ratio, while maintaining other molar ratios constant, was also investigated. The reaction degree was calculated from the decomposition of ^{29}Si spectra to understand the influence of H_2O/Na_2O ratio and slag incorporation on the compressive strength.

2. Materials and methods

2.1. Materials and sample preparation

The metakaolin used in this study was produced by the flash calcination of kaolin from Fumel, France. It mainly consists of silica (67.1 wt. %) and alumina (26.8 wt. %). The high silica content of metakaolin is due to significant proportion of quartz. Its proportion of pure metakaolin $Al_2O_3(SiO_2)_2$ phase was 43% [31]. The chemical and physical properties of metakaolin and ground granulated blast furnace slag (GGBFS) are described in Table 1.

Table 1. Chemical composition (mass fraction. %) and properties of metakaolin and slag.

(wt.%)	métakaolin	slag
SiO_2	67.1	37.2
Al_2O_3	26.8	10.5
CaO	1.12	43.2
Fe_2O_3	2.56	0.6
MgO	0.11	7.0
SO_3	-	0.1
Cl^-	-	0.01
TiO_2	1.3	0.5
Na_2O	0.01	0.6
Median diameter d_{50} (µm)	18	10
Specific surface BET ($m^2.g^{-1}$)	16.5	0.45
Density	2.63	2.90

The activation solution was prepared by diluting a sodium silicate solution with a fixed SiO_2/Na_2O ratio of 1.7 and 44% dry content in demineralized water. It is noteworthy that the sodium silicate solution was specially designed with relatively high Na_2O content, in order to reduce as much as possible the subsequent addition of NaOH during the preparation of AAMs. A very low sodium hydroxide NaOH content was actually added in pellets to adjust the Na/Al ratio to 1. The molar ratio of SiO_2 to Na_2O in the activator and the chemical compositions have been chosen as recommended in the literature to allow a good dissolution

of the precursor [32]. Therefore, the total NaOH content in activating solution includes equivalent NaOH from the sodium silicate solution deduced from its Na_2O molar content, and NaOH in pellets. The alkali-activated mixtures were designed to obtain the stoichiometry of the systems detailed in Table 2. Molar ratios were calculated considering the initial chemical composition of the sodium silicate solution, added NaOH, the amorphous fraction of the metakaolin, and slag. Activated metakaolin systems have been designed with constant Si/Al, Na/Al atomic ratios and different H_2O/Na_2O molar ratios.

Table 2. Compositions of the studied mixtures

Mixtures		**MK21**	**MK34**	**MKS21**	**MKS34**
Materials	**Density**	**Compositions (g/l)**			
Metakaolin	2.63	732	518	562	397
Slag	2.9	-	-	187	133
Na-silicate	1.55	636	450	636	450
NaOH pellets	1.46	3.3	2.3	3.3	2.3
Bentonite	2.5	9	15	9	15
Dispersant	1.4	5.5	4	5.5	4
Water	1	310	511	310	511
Water to solid ratio (W/S %wt.)		0.65	1.04	0.65	1.04
Volume fractions (%)					
Water		66	76	66	76
Solid phases		34	24	34	24
Atomic ratios					
Si/Al		1.83	1.83	2.20	2.20
Na/Al		1	1	1.1	1.1
Molar ratio					
H_2O/Na_2O		21	34	21	34
Total NaOH in activating solution (mol/l solution)		5.29	3.25	5.29	3.25

Binary metakaolin-slag mixtures were derived from 100% metakaolin mixtures. Metakaolin was replaced by 25 %wt of slag at constant volume. The water to solid ratio is calculated from the total water in the mixture, including the added demineralized water and the water fraction in the activation solution, and the total amount of solid including the precursor and the solid fraction of the activation solution. The total NaOH in activating solution takes into account NaOH from the sodium silicate solution and added NaOH pellets. The total NaOH concentration decreased with water-to-solid ratio but remained relatively high. Based on a previous study [33], bentonite and dispersant were added for the stabilization and deflocculation of particle suspensions respectively. Regarding the mixing procedure, the powders were added to the activating solution and stirred in a high shear mixer for 5 minutes to ensure a proper homogenization. The specimens characterized at hardened state were sealed and stored at 20°C.

2.2.Test methods

2.2.1. Compressive strength

The compressive strength testing was carried out on a 100kN press. The load rate was 1.9kN/s until failure. Compression tests were performed at the ages of 7, 28 and 90 days on cylinders with a diameter of 7 cm and a height of 14cm.

2.2.2. Nuclear magnetic resonance (NMR)

Solid-state ^{29}Si NMR spectroscopy was performed using a Bruker Avance III 300 MHz (7 T) spectrometer and a 7mm MAS probe, and ^{27}Al magic angle spinning (MAS) NMR spectroscopy was performed on a 500 MHz Bruker Avance III using a 2.5mm MAS probe. For ^{27}Al acquisition, the MAS speed was 30 kHz and the repetition time was set to 1s. The ^{27}Al spectra were carried out with a single $\pi/13$ excitation pulse for a radiofrequency field of 12 kHz. Chemical shifts were referenced against $Al(NO_3)_3$ solution. For ^{29}Si acquisition, the

MAS speed was 5 kHz. The ^{29}Si MAS NMR spectra were acquired with single $\pi/2$ excitation of 5.5 µs. The recycle delay between scans was set to 5s. Chemical shifts were referenced against TMS.

2.2.3. X-ray diffraction (XRD)

XRD is mainly used to describe crystallized phases. Geopolymers are mainly amorphous so XRD is relevant to investigate the consumption of primary alumino-silicate phases and to detect the apparition of new crystallized phases. The X-ray diffractograms were obtained from a Bruker AXS D8 Advance diffractometer, equipped with an anticathode tube made of copper (Cu-Kα : λ = 1.5418 Å). Voltage and current were set to 40 kV and 40 mA. Disoriented powders diffractograms were recorded between 2°2θ et 60°2θ with a step equal to 0,017°2θ and a measuring time of 1 second per step. Diffractograms were analyzed thanks to EVA software from Bruker and the Crystallography Open Database.

3. Results and discussion

3.1. Mechanical properties

Figure 1 shows the compressive strength development of activated metakaolin and activated metakaolin-slag mixtures at 7, 28, and 90 days respectively. The binary mixtures developed significantly higher strength than plain metakaolin system at the same H_2O/Na_2O ratio. This is consistent with previous results reporting that adding slag to activated metakaolin has a positive effect on the development of mechanical strength [21] [23]. A drop in strength can be observed when increasing H_2O/Na_2O ratio to 34 in both activated metakaolin and metakaolin-slag mixtures. The compressive strength of MK21 was around 19 MPa after 90 days whereas the strength of MK34 was still not measurable. Increasing H_2O/Na_2O leads to lower strength and higher porosity as water affects density and open porosity [34] [35]. Additionally, the composition and the structure of the reaction products can be changed depending on the

amount of water available in the system and the concentration of alkali cations [29], [36], [37] but the experimental data related to the effect of water with constant molar ratios are scarce.

Compressive strength of studied mixtures increased from 7 to 90 days. This can be attributed to reaction advancement and/or microstructure evolutions. Chen et al. [38] quantitatively correlated the degree of reaction related to the amount of gel formed with the compressive strength of metakaolin-based geopolymers with and without calcium. Cherki El Idrissi et al. [16] showed that the mechanical properties of metakaolin-based materials highly depend on the changes in local structures. However, it is still not clear how slag and water content modify the reactivity of precursors and the structure of formed products. X-ray diffraction was used to analyze the formation of crystalline materials if any. Additionally, the local structure was investigated for all mixtures using ^{29}Si and ^{27}Al NMR spectroscopy to understand the effect of H_2O/Na_2O ratio and slag incorporation on binding phase and to estimate the reaction degree at different curing times.

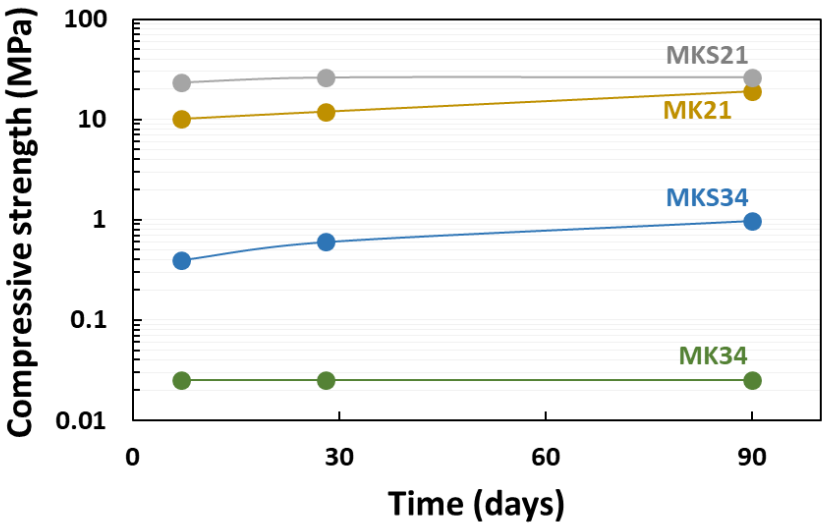

Figure 1. Compressive strength development of different mixtures at 7, 28 and 90 days

3.2. Phase composition

3.2.1. X-ray diffraction (XRD)

Figure 2 represents the XRD patterns of different mixtures at different ages. The major crystalline phase is quartz (SiO_2) originating from raw metakaolin. The carbonation of slag hydration products in binary mixtures can contribute to calcite formation. Calcite could be detected in MK21 at 28 days despite the low Ca content in metakaolin. Anatase (TiO_2) and kaolinite $Al_2Si_2O_5(OH)_4$ observed in all samples originated from the raw materials.

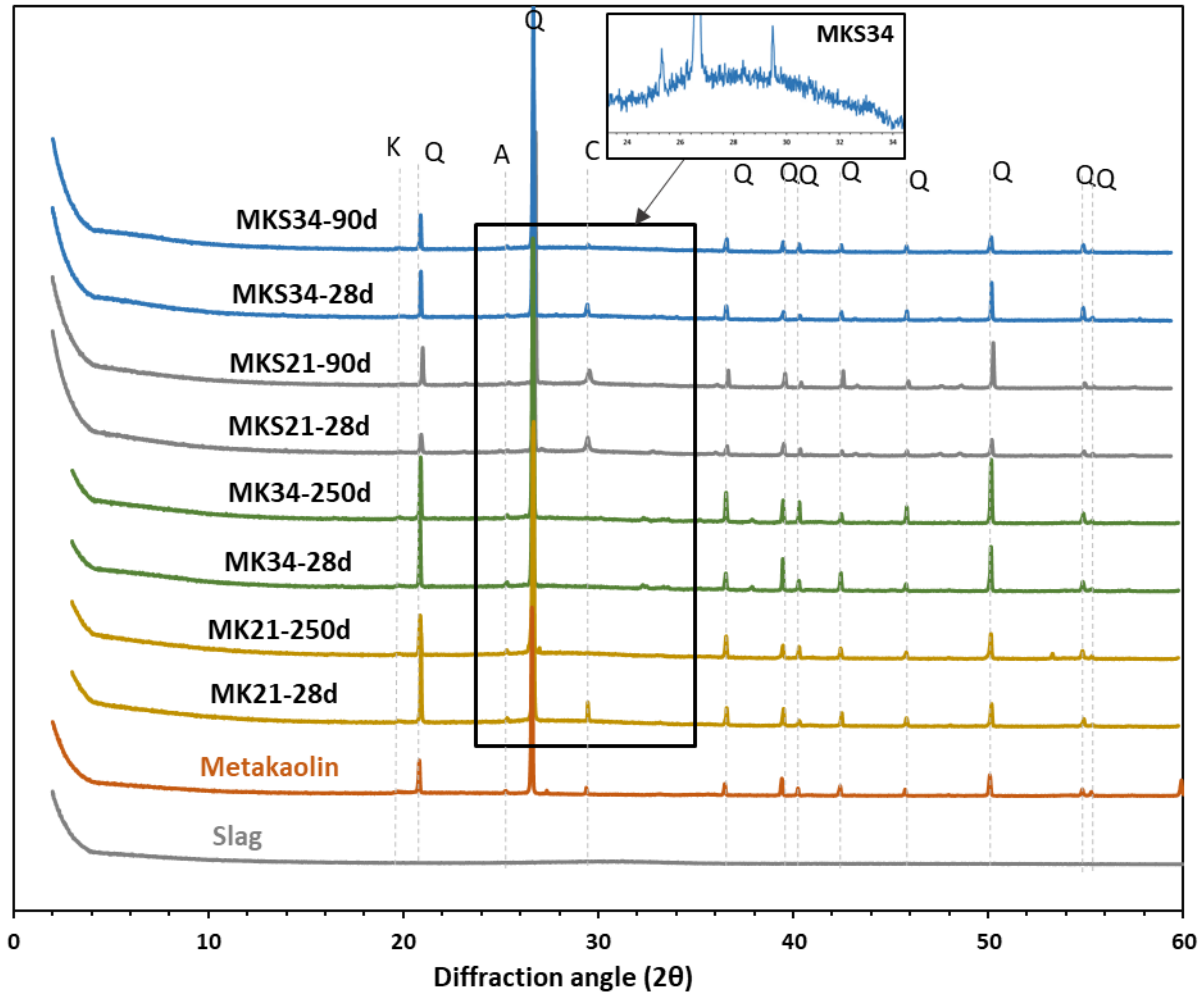

Figure 2. XRD patterns of different mixtures,

C: calcite; Q: quartz, A: Anatase, K: Kaolinite

New crystalline products could not be detected except calcite. A broad hump can be observed between 2θ=25° and 2θ=35°. This implies that all the products, which are specific to reactions involving sodium silicate, metakaolin and slag, are very poorly crystalline. This hump in such mixtures is often associated with the geopolymer products [39] whose crystalline domains can be of about 5 nm [27], which is below the detection limit of XRD. It is noteworthy to mention that adding slag to the mixtures did not result in the formation of new crystalline phases. However, the hump at 2θ=30° can be attributed to an aluminum substituted tobermorite-like phase ($Ca_5Si_5Al(OH)O_{17}.5H_2O$,) [7]. This phase is expected to be formed in such mixtures [16], [22], [26], [30], [40]. It is although mostly amorphous and can be integrated into the amorphous hump mentioned above.

3.2.2. ^{27}Al NMR analyses

^{27}Al NMR spectra of the raw metakaolin and activated mixtures cured for 28 and 250 days are presented in Figure 3. Raw metakaolin exhibits three overlapping peaks with maxima at 55 ppm, 28 ppm, and 4 ppm according to four, five, and six-coordinated aluminum, respectively. The width of these peaks reflects the amorphous character of the metakaolin attributed to dehydroxylated kaolin. The slag spectrum shows broad overlapping peaks attributed to a variety of aluminum environments with a majority of Al(IV). All activated mixtures spectra showed a main resonance with a maximum between 58 and 60 ppm that corresponds to tetrahedral sites AlO_4(4Si) type in aluminosilicate glasses [41]. The variation of H_2O/Na_2O did not significantly influence the position of the main resonance peak in both types of mixtures.

In the activated metakaolin systems, the predominant signal centered around 58 ppm corresponds to tetrahedrally coordinated aluminum in the reaction products forming a three-dimensional silico-aluminate framework, in agreement with previous observations of

aluminosilicate-based geopolymers [15], [42], [43]. Significant spectral intensity below 40 ppm (Al^{V} and Al^{VI} signals) indicates that a higher amount of metakaolin did not react at higher H_2O/Na_2O.

Small variations in the shielding of the resonances are observed by comparing binary metakaolin-slag systems to activated metakaolin mixtures. The ^{27}Al chemical shifts may be affected by geometric factors such as T-O-T angles (where T is Si or Al) or the type of cations in more distant coordination spheres [29] [44]. Walkley et al. [44] reported that the incorporation of Sr^{2+} and Ca^{2+} at a low concentration displaces some of the alkali cations Na^{+} and K^{+} from the extra-framework sites and fulfill the charge balancing role. It was found that adding calcium to the metakaolin system results in a slight shift from 56.6 ppm to 57.9 ppm in ^{27}Al NMR spectrum [45]. Ca^{2+} can be taken up in the 3D aluminosilicate network and compensate the negative charge after the replacement of Si^{4+} by Al^{3+} [45]. The incorporation of slag in the system also resulted in a slight increase in the full width at half height (FWHH). This observation is consistent with a recent study reporting an increase in the FWHH of the AlO_4 resonance as the calcium content increases in the mixtures can be explained by the higher Ca^{2+} uptake in the aluminosilicate structure [27].

Nevertheless, Bernal et al. [46] mentioned that the resonance in fly ash–slag mixtures, which is somewhat broader than solely fly ash, is comprised of a contribution at a high chemical shift from the C-A-S-H gel and another at a lower chemical shift from the N-A-S-H gel. Both phases would contain Al in significantly distorted tetrahedral environments, which lead to the broad resonance centered around 58 ppm [46] [40].

In our study, binary mixtures and plain metakaolin systems showed a slight difference in the position, shape and width of ^{27}Al spectrum. Further information on the short-range order of the silicate tetrahedral is presented in the following section.

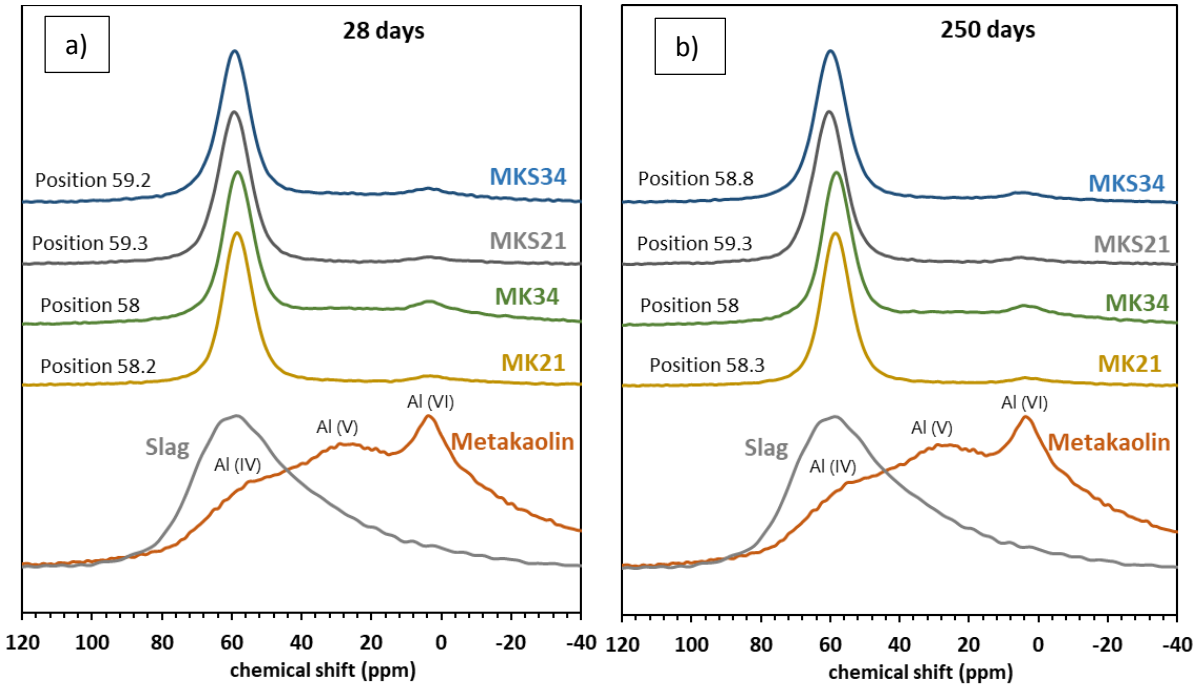

Figure 3. ^{27}Al MAS NMR spectra of raw metakaolin, raw slag and activated systems at 28 and 250 days

3.2.3. ^{29}Si NMR analyses

Figure 4 shows the ^{29}Si MAS NMR spectra of the raw metakaolin, raw slag, and sodium silicate activated mixtures. The broad asymmetric resonance width is indicative of the amorphous structure of these materials. Raw metakaolin spectrum presents a main peak with a maximum at -99 ppm. The peak detected at -107 ppm comes from the quartz present in raw metakaolin [16]. The spectrum of raw slag lies in a variety of Q^0, Q^1, and Q^2 sites, mostly Q^0 resulting in a peak maximum around -75 ppm.

Activated metakaolin systems presented a broad resonance with a maximum between -91 ppm and -93 ppm regarding H_2O/Na_2O ratios. A shift of the overall ^{29}Si spectra to lower frequencies is observed at high H_2O/Na_2O ratio. However, this resonance in the ^{29}Si spectra is mainly attributed to the Q^4 type environment and its width is explained by the presence of the Q^4(mAl) type environment with m varies between 0 and 4 [16] [42]. This is in accordance

with the observed ^{27}Al spectrum (Figure 3) where the large peak centered at 58 ppm comes from the four-coordinated aluminum Al (IV) in geopolymer structure. In agreement with previous section, the shoulder in resonances at about -100 ppm, more intense in the mixture with higher H_2O/Na_2O ratios, confirms the remnant metakaolin in the activated metakaolin systems at 28 and 250 days (detailed in the following section). The residual quartz present in raw metakaolin can be also detected at -107 ppm.

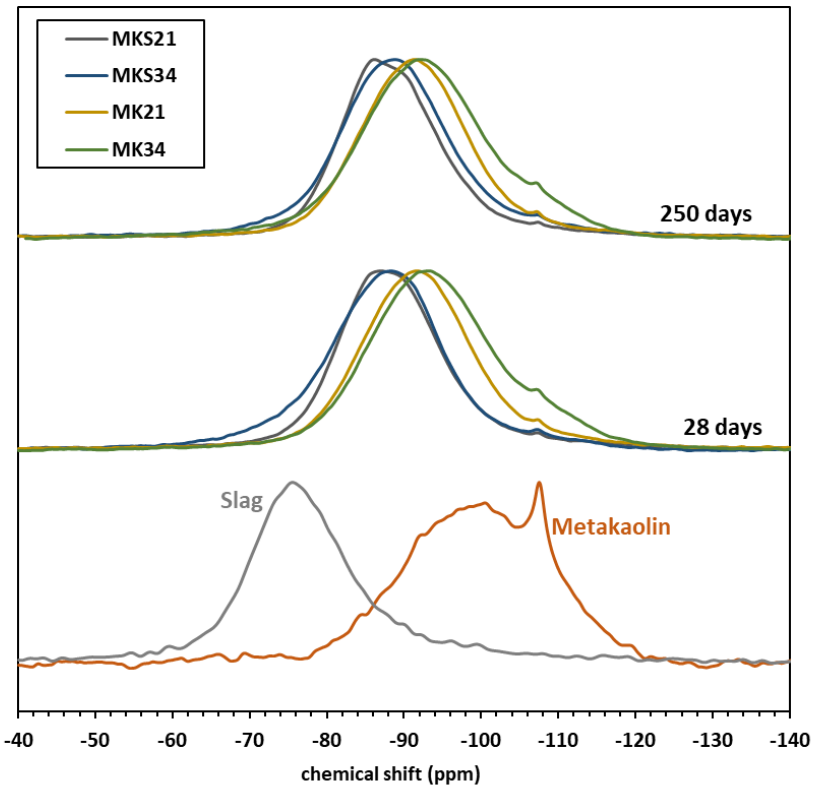

Figure 4. ^{29}Si MAS NMR spectra of raw metakaolin, raw slag and activated systems

In binary mixtures, spectra shifted to higher frequencies in comparison with plain metakaolin mixtures (between -72 ppm and -110 ppm). The main resonance peaks between -91 ppm and -93 ppm observed in plain metakaolin mixtures shifted to -87 ppm and -89 ppm. The ^{29}Si spectrum of the mixture MKS34 shifted to slightly higher frequencies than the mixture MKS21, probably due to the remnant metakaolin. It is noteworthy to mention that after 250 days, the intensity of the shoulder observed at -76 ppm in the mixture MKS34 decreased,

implying a further dissolution of slag in function of the time. A sharp peak in MKS21 after 250 days appeared at -86 ppm. This can indicate a structural organization of the product phase with curing time.

The broad width, in binary mixtures, indicates the presence of Si in different environments of type Q^n(mAl), where n is the coordination number of the silicon center and m is the number of aluminum atoms neighbors ($0 \leq n \leq m \leq 4$). Based on the literature, chemical shifts between -75 ppm and -94 ppm can be referred to Q^1, Q^2, Q^2(1Al), Q^3(1Al), and Q^3sites in an Al substituted C-S-H type (C-(A)-S-H) gel with a tobermorite type structure [16]. These sites can overlap with Q^4 type environment (often detected between -88 ppm and -109 ppm [16] [42]) with Al uptake by the alkali-aluminosilicate gel network expected to be formed in such mixtures. Different studies concluded on the presence of two distinct intermixed gels in activated blends [30] [22]. Buchwald et al. [20] reported the presence of geopolymer and hydrated slag binder in different proportions depending on their composition in a metakaolin-slag material.

On the other hand, the coexistence of N-A-S-H and N-(C)-A-S-H, both with a 3D network structure, intermixed with C-A-S-H have been identified in alkali-activated metakaolin-limestone cement [27]. This observation is in agreement with the results on the calcium metakaolin activated system evoked in [38] [26] [45]. The simultaneous presence of C-A-S-H with a 2D structure and Q^1 and Q^2 sites, intermixed with a calcium modified geopolymer gel that has 3D structure with Q^3 and Q^4 sites, and with an aluminosilicate gel N-A-S-H with Q^4 sites were identified in [38] [26]. Adding calcium to an aluminosilicate system resulted in an uptake of calcium into N-A-S-H gel with a preserve of the 3D structures [44] [45]. It was suggested that Ca^{2+} uptake into N-(C)-A-S-H happens through an ion-exchange mechanism in which Ca^{2+} displaces Na^+ after the formation of N-A-S-H [17] [27]. The transition from a 3D structure towards a linearly structured one depends on the availability and form in which the

Ca, Na, Si, and Al are supplied [27]. Lodeiro et al. [17] have proposed a model for the stability of N-A-S-H gel as function of pH and Ca concentration.

Based on this, intermixed gels can be expected in the studied materials. It is noteworthy to mention that the identification of the coexisting phases and their respective proportions are key data to understand their macroscopic properties, such as strength and durability. The reaction products formed in this experimental study are discussed in detail in the following section by taking into account the dispersed opinions discussed the role of calcium. The results related to a set of initial assumptions allow discussing their relevance. ^{29}Si spectra have been deconvoluted using Dmfit free software to perform spectral simulations [47]. Therefore, a quantification of the resonance species have been achieved and the reaction degree of metakaolin and slag and the overall degree of reaction have been then calculated to understand the effect of both slag incorporation and H_2O/Na_2O ratio on the reaction advancement and the phase composition.

3.3. Towards the quantification of reaction products

The ^{29}Si spectra are deconvoluted using a series of Gaussian peaks to simulate resonances using a least-square fitting method which is routinely performed in the study of alkali-activated materials. In all spectra deconvolutions, congruent dissolution of slag and metakaolin is assumed [44] [20]. The contribution of the remnant metakaolin is considered by fitting a scaled component spectrum calculated from the ^{29}Si MAS NMR spectrum of raw metakaolin and raw slag, respectively. Raw metakaolin is represented by a Gaussian signal centered at -99 ppm. The contribution of quartz around -107 ppm has not been considered because of the very long relaxation delays associated with the Q^4 sites in quartz which means that they will not be captured quantitatively in the spectra here. Additionally, the quartz reactivity is neglected thus it is not taken into account in the advancement of the reaction.

Three approaches are used to analyze and quantify the reaction products and the remnant precursors (Table 3). The Gaussian lines used for the decomposition of ^{29}Si spectra are usually defined by their intensity, the peak position, and the full width at half height (FWHH).

Table 3. Different methods used: Assumptions and variables

Method	Assumptions	Variables (Gaussian model)	References
1	One phase representing the reaction product	Peak position / FWHH/ Intensity	
2	Two distinct phases are formed Phase 1 Phase 2	Peak position / FWHH / Intensity	
2-bis	Two distinct phases are formed Phase 1	Peak position / FWHH/ Intensity	[22], [30], [46], [20]
	Phase 2 : Geopolymer GP	Intensity (Peak position and FWHH are maintained constant as plain metakaolin mixture)	
3	Deconvolution of reaction products using the minimum possible number of component peaks to represent mainly a 3D network structure	Intensity (Peak position : fixed from literature FWHH : constant for all the deconvoluted spectrum and <7ppm)	[27]

The first method, which is the simplest one, consists of the decomposition of the overall spectrum into three signals: remnant metakaolin, remnant slag (in binary mixtures), and a Gaussian signal representing the formed phase as presented in Figure 5. This deconvolution was conducted on all the mixtures. The results are given in Table 4. The formed phase in metakaolin system is centered between -90.9 ppm and -91.3 ppm at different ages. It shows that the shift in the overall ^{29}Si spectra (1 ppm to 2 ppm) is only an apparent shift as it results from the higher contribution of unreacted metakaolin overlapping with the peak of the

geopolymer formed which remains at the same position whatever the water content. This implies that water does not change the structure of the reaction product, i.e. a geopolymer structure is formed whatever H_2O/Na_2O ratios. A more notable difference in binary mixtures in the position of the reaction product can be observed by varying H_2O/Na_2O ratio. In the binary mixtures, the product shifts to higher frequencies compared to the geopolymer phase in activated metakaolin. Increasing water content leads to a lower dissolution of precursors due to its diluting effect and therefore a lower fraction of the binding phase. A high amount of unreacted metakaolin and slag, if any, can be detected at a high H_2O/Na_2O ratio. An increase in H_2O/Na_2O ratio results in a lower available OH^- concentration and limited dissolution of precursor, thus less aluminate and silicate monomers can participate in polymerization. Moreover, the dissolution of the aluminosilicate source and the ionization process consume hydroxides. Thus, the availability of hydroxides continuously decreases.

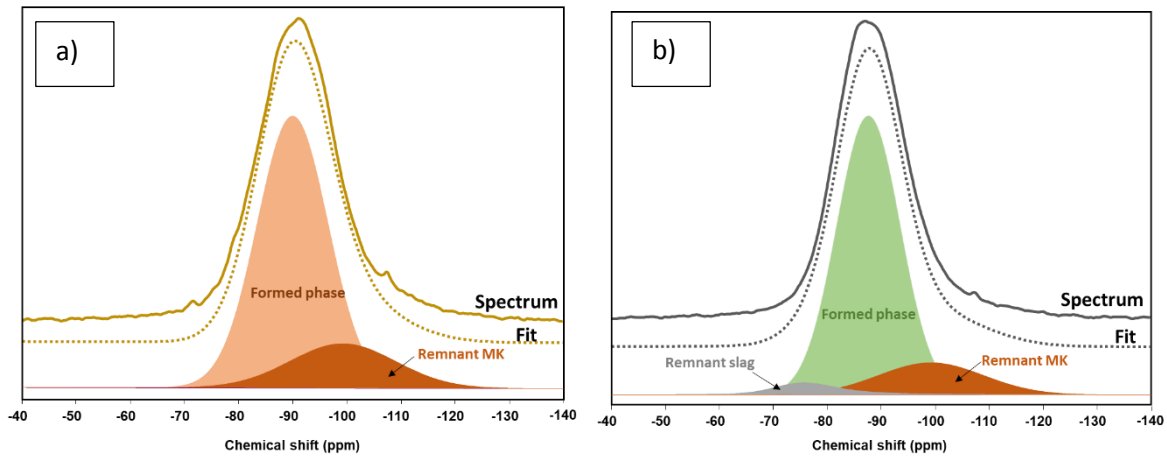

Figure 5. Decompositions of the ^{29}Si MAS NMR spectra of a) activated metakaolin MK21 and b) activated metakolin-slag MKS21 at 28 days using *method 1*

Table 4. Analysis of ^{29}Si NMR spectra using method 1

Mixtures		Remnant Slag mol-%Si	Remnant Metakaolin mol-%Si	Product Position (ppm)	Product FWHH	Product mol-%Si
MK21	**28 d**	-	20	-90.9	15.6	80
	250 d	-	17	-90.6	15.1	83
MK34	**28 d**	-	45	-91.3	15.5	55
	250 d	-	37	-90.7	16.4	63
MKS21	**28 d**	5	15	-87.6	13.9	80
	250 d	0.4	14	-87.5	13.7	85
MKS34	**28 d**	12	21	-88.4	13.9	67
	250 d	9	19	-88.3	13.9	72

Method 2 is based on previous studies reporting the presence of two distinct phases N-A-S-H and C-A-S-H in a blended material [20] [30] [15] [29] [22]. Thus, two Gaussian lines associated with the two-formed phases were used to obtain the best fit of the overall spectrum (Figure 6). Table 5 summarizes the obtained results. Phase 2 is in the region of Q^4(mAl) sites which defines a geopolymer structure whereas Phase 1 falls into the range of C-(A)-S-H gel at higher frequencies. The formation of Phase 1 is favored at a lower H_2O/Na_2O ratio with a preponderance of Phase 2 whatever the ages and the water content. By comparing Phase 2 to the formed phase in activated metakaolin material, there is a slight change in the position and the full width at half height decreases to 12. This suggests that the geopolymer structure has been modified by the incorporation of slag or that the method used does not allow assessing the real phase composition. Method 2 was modified (method 2-bis) by keeping the decomposition of the binding phase into two signals but here the phase 2, which represents the geopolymer, was directly extracted from the phase formed in the corresponding plain metakaolin mixture (MK21 at 28 days) at the same age and water content. The position and the width of phase 2 in MKS21 was fixed to -90.9 ppm and 15.6 respectively deduced from MK21 at 28 days (Table 4). Figure 7 shows the spectral deconvolution.

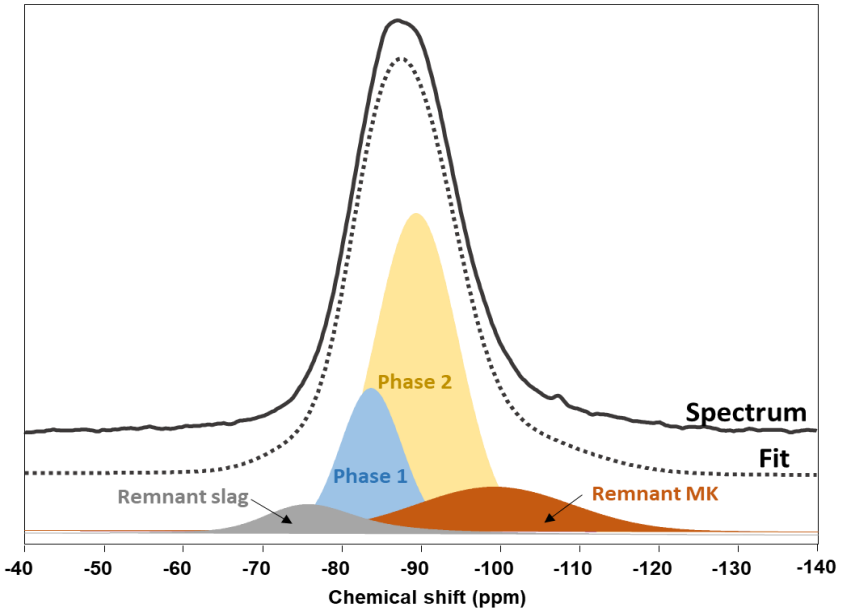

Figure 6. Decomposition of the ^{29}Si MAS NMR spectrum of activated metakolin-slag MKS21 at 28 days using *method 2*

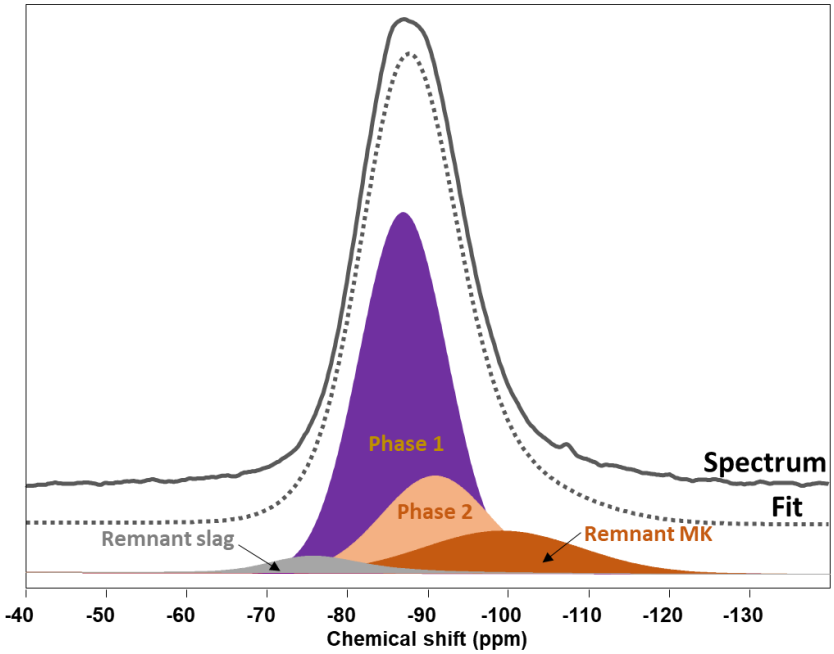

Figure 7. Decompositions of the ^{29}Si MAS NMR spectrum of activated metakolin-slag MKS21 at 28 days using *method 2-Bis*

The contribution of the geopolymer signal (phase 2) in the overall spectrum is surprisingly low compared to phase 1. Phase 1 is centered at -87 ppm and lies in the range of Q^1 to Q^4 sites. These results are in accordance with results obtained in a recent study on activated metakaolin containing calcium [26] [38]. It was suggested that a calcium-modified geopolymer (Ca,Na)-S-H with a three-dimensional structure was formed and presented a

Si/Al ratio lower than the conventional C-A-S-H gel with chain structures [38]. However, they reported that the 3D modified structure could not be presented directly from peak positions in the spectrum because the Q^4 peaks associated with three-dimensional structures would overlap with the sites on low frequencies associated with chain structures [38].

Table 5. Analysis of ^{29}Si NMR spectra using method 2 for binary mixtures

Mixtures		Remnant Slag mol-%Si	Remnant Metakaolin mol-%Si	Phase 1			Phase 2		
				Position (ppm)	FWHH	mol-%Si	Position (ppm)	FWHH	mol-%Si
MKS21	28 d	8	15	-83.7	9.0	19	-89.4	12.3	58
	250 d	6	14	-84.4	9.4	29	-90.0	12.1	51
MKS34	28 d	15	23	-82.9	8.0	4	-88.5	12.8	58
	250 d	12	18	-83.6	9.0	10	-89.4	12.9	60

Method 3 associates a Gaussian signal with each Q^4(mAl) site following Engelhard's notation [49]. Gaussian line model was used for deconvolution of ^{29}Si MAS NMR spectra using the minimum possible number of component peaks to describe accurately the spectrum. The full width at half-height (FWHH) and peak positions were kept constant throughout all spectral deconvolutions whenever possible. Peak locations were defined based on the available literature [20] [27] [50] [46]. Finally, the area of each component in ^{29}Si MAS NMR spectra represents the relative concentration of each Si species. ^{29}Si spectrum of binary mixtures is deconvoluted based on the study of Peres Cortes et al. [27] wherein an intermixed gel of sodium aluminosilicate hydrate (N-A-S-H) and sodium (calcium) aluminosilicate hydrate N-(C)–A-S-H with 3D network structures are formed in an alkali-activated metakaolin limestone cement. The resonances at -84.9, -89.7, -93.8, -98.3, and -103 ppm were attributed to Q^4 SiO_4 species coordinated with 4, 3, 2, 1, and 0 AlO_4 tetrahedral, respectively. The resonance at -78.1 and -79.9 ppm were associated with Q^1 and Q^2(1Al) species respectively. The peak at -

84.9 ppm that can overlap with Q^2 and Q^3(1Al) signals is assigned to Q^4(4Al) considering the significant intensity for AlO_4 species at 54-57 ppm observed by ^{27}Al MAS NMR [27].

Figure 8 shows that the peaks used to fit the ^{29}Si NMR spectra of the binary mixtures. The quantification of the different Q^n(mAl) species of binary mixtures is shown in Table 6. The equation for calculating the Si/Al molar ratio from Engelhard's formula [49] (Equation **(1)**) is used to determine the Si/Al ratio of the binding phase:

$$\frac{Si}{Al} = \frac{\sum_{n=0}^{4} Q^4(nAl)}{\sum_{n=0}^{4} \frac{n}{4} Q^4(nAl)} \qquad (1)$$

As a result, the amount of Q^2 species is relatively low compared to Q^4 species. The peak associated with Al-rich structural units Q^4(4Al) and Q^4(3Al) presented higher intensities at the expense of the Si-rich structural unit peaks. Thereby, a predominance of Al-rich structural units in the reaction products can be concluded. It is noteworthy to mention that this conclusion is always right by considering the hypothesis and the peak shifts attributed for each Si environment of method 3 as described above. However, a change of the signal attribution at -84.9 ppm for Q^2 and Q^3(1Al) signals would be enough to change the retained conclusions. In addition, a fit with a single component Q^2(1Al) is not representative of the gel 'C-A-S-H'. If there were only Q^2(1Al), the Si/Al ratio would be equal to 1 which is under the lower boundary of the conventional C-A-S-H [51] , there are necessarily Q^1,Q^2, and Q^3(1Al). In other words, some issues related to the deconvolution method imply remaining cautious about the results.

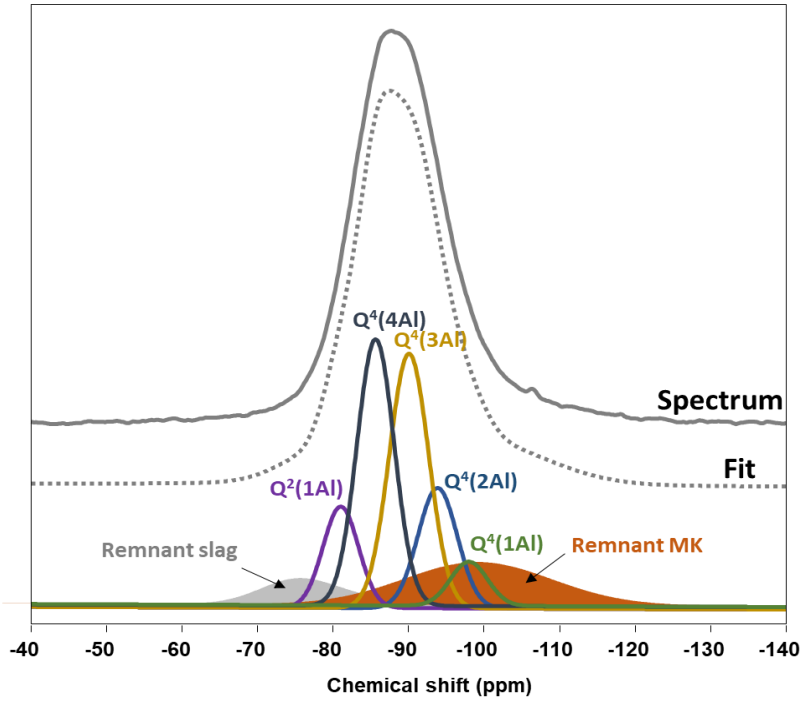

Figure 8. Decompositions of the ^{29}Si MAS NMR spectrum of activated metakaolin-slag MKS21 at 28 days using method 3

The Si/Al ratio of all mixtures lies between 1.28 and 1.33 (Table 6). These values are lower than that of the initial composition mixtures indicating preferential precipitation of an Al-rich gel. Increasing H_2O/Na_2O ratio resulted in a slight increase in Si/Al for the different formulations. Compared to the mixtures with a lower H_2O/Na_2O ratio, mixtures with a high H_2O/Na_2O ratio had higher remnant metakaolin, slag, and thus a lower percentage of reaction products. The amount of AlO_4 coordinated to SiO_4 was thus reduced due to a lower dissolution of precursors leading to a lower Al uptake in the binding phase. On the other hand, the trend of the variation of Si/Al in function of time is not clear. It is difficult to conclude on significant differences and evolutions. A small change of the signal attribution could modify the value of Si/Al. This underlines once again the issues related to the deconvolution method.

Table 6. Analysis of ^{29}Si NMR spectra using method 3 for binary mixtures

Position Gi (ppm) / mol-%Si		Remnant Slag	Remnant Metakaolin	Q^1 -78.14	Q^2(1Al) -79.9	Q^4(4Al) -84.9	Q^4(3Al) -89.7	Q^4(2Al) -93.8	Q^4(1Al) -98.3	Q^4(0Al) -103.6	Si/Al
MKS21	**28 d**	8	15	0	9	27	25	12	4	0	1.29
	250 d	5	14	0	9	29	27	12	4	0	1.28
MKS34	**28 d**	14	22	0	7	21	23	9	4	0	1.29
	250 d	12	19	0	7	22	24	12	4	0	1.33

The overall degree of reaction (RD_{ov}) can be determined from the amount of each phase formed in terms of Si mol%. It can be computed as Si mol% in the product with respect to that in the entire sample corresponding to product phase and unreacted metakaolin and slag (Equation **(2)**). The reaction degree is therefore equivalent to the amount of product.

$$RD_{ov}(Si) = \frac{\boldsymbol{Moles\ of\ Si\ in\ product\ phase}}{\boldsymbol{Moles\ of\ total\ Si\ in\ sample}} \qquad \textbf{(2)}$$

The reaction degree of metakaolin RD_{mk} (Equation (**3)**) and slag RD_s (Equation (**4)**) can be calculated separately. $\boldsymbol{X(Si)_{mk}}$ and $\boldsymbol{X(Si)_s}$ refer to the silicon provided by metakaolin and slag respectively and determined from their chemical composition (Table 1). Only the amorphous fraction of the metakaolin is considered in the calculation.

$$RD_{mk} = \frac{\boldsymbol{X(Si)_{mk} - R_{mk}}}{\boldsymbol{X(Si)_{mk}}} \qquad \textbf{(3)}$$

$$RD_s = \frac{\boldsymbol{X(Si)_s - R_s}}{\boldsymbol{X(Si)_s}} \qquad \textbf{(4)}$$

The results are given in Table 7. It can be concluded that the decomposition methods mostly agree with each other in terms of reaction degree. Nevertheless, the challenge lies in the representation of the products. In Figure 9, an average value and the difference between the three methods are represented with a difference between the minimum and the maximum values.

Table 7 Reaction degrees provided by the different methods

Mixtures	Days	Method 1			Method 2			Method 3		
		RD_{mk}	RD_s	RD_{ov}	RD_{mk}	RD_s	RD_{ov}	RD_{mk}	RD_s	RD_{ov}
MK21	**28**	63	-	80	-	-	-	-	-	-
	250	68	-	82	-	-	-	-	-	-
MK34	**28**	17	-	54	-	-	-	-	-	-
	250	32	-	63	-	-	-	-	-	-
MKS21	**28**	61	73	80	62	56	77	61	54	77
	250	64	98	85	65	67	80	65	70	82
MKS34	**28**	46	32	67	43	10	62	44	16	63
	250	53	47	72	54	32	70	51	29	69

Figure 9 shows the reaction degree of the different mixtures. MK21 and MKS21 present a higher reaction degree than high H_2O/Na_2O mixtures. Replacing a part of metakaolin by slag slightly changes the overall reaction degree but it influences differently the reactivity of metakaolin depending on the H_2O/Na_2O ratios. At low water content, the reactivity of metakaolin does not seem to be influenced by the addition of slag to the mixture. The overall reaction degree reached 80 % and the reaction degree of metakaolin was 63% and 61 % in MK21 and MKS21 at 28 days respectively. These values slightly increased after 250 days. A different trend can be noticed at a higher H_2O/Na_2O ratio. Replacing metakaolin by slag in MK34 increased the reactivity of metakaolin from 17% to 44 %. It would mean that slag enhanced the dissolution of metakaolin; however, the overall reaction remained low. This is consistent with previous study stating that adding calcium to the metakolin systems enhanced the dissolution of metakaolin and increased the reaction degree [38] [26] [20]. The formation of C-A-S-H at early age of reaction in a calcium-rich medium consumes silicate in the pore solution, which enhances the dissolution of metakaolin to sustain the silicate concentration leading to a release of aluminates [52] [53]. Besides, the formation of C-A-S-H also consumes water, which increases the alkalinity of the system and further enhances the dissolution of precursor [53]. As calcium reduces silicate in solution, the protective layer of aluminosilicate

gel, which forms on metakaolin surface mainly in the silicate-activated mixes [54], is less likely to form and limit further dissolution.

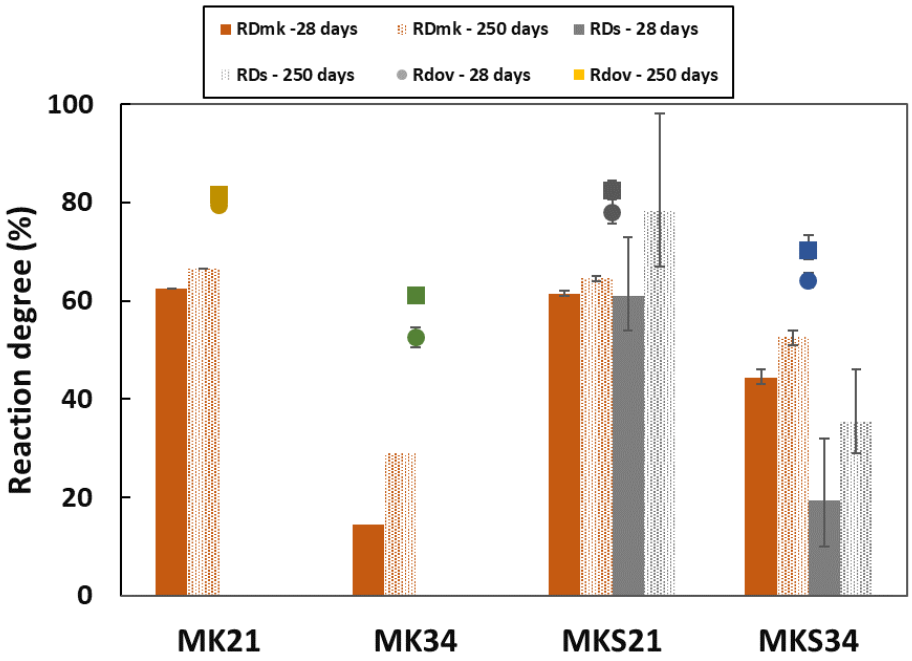

Figure 9. Comparison of reaction degree, calculation from ^{29}Si NMR spectroscopy; the error bars represents the difference between the methods used

Finally, compressive strength at 28 days is plotted versus the reaction degree Si mol% (RD_{ov}, RD_{mk}, RD_s) (see Figure 10). It was reported that compressive strength is linearly correlated with the reaction degree [38]. However, the compressive strength in our study does not seem to be linearly correlated with the degree of reaction. MK21 and MKS21 exhibited similar reaction degrees (RD_{ov} , RD_{mk}) whereas they developed different compressive strengths. The strength does not only depend on reaction degree but also on the proportion of solid phase and microstructural parameters. The solid phase content depends on initial proportion of solid reactants and chemically bound water. The combination of C-A-S-H and calcium-modified geopolymer gel produces strength more efficiently than mixtures containing only plain geopolymer gel. The positive effect of adding calcium on compressive strength was reported previously [23] [38] [27]. At high H_2O/Na_2O, the slight increase in compressive

strength of MKS34 compared to MK34 is due to both the increase in the reactivity of metakaolin and the presence of calcium in the mixture. However, both the reactivity of metakaolin and slag are influenced by high water content. This could suggest similar factors affecting the initial dissolution of precursors that prevent further dissolution at high water content and the mechanism of formation of the product phase.

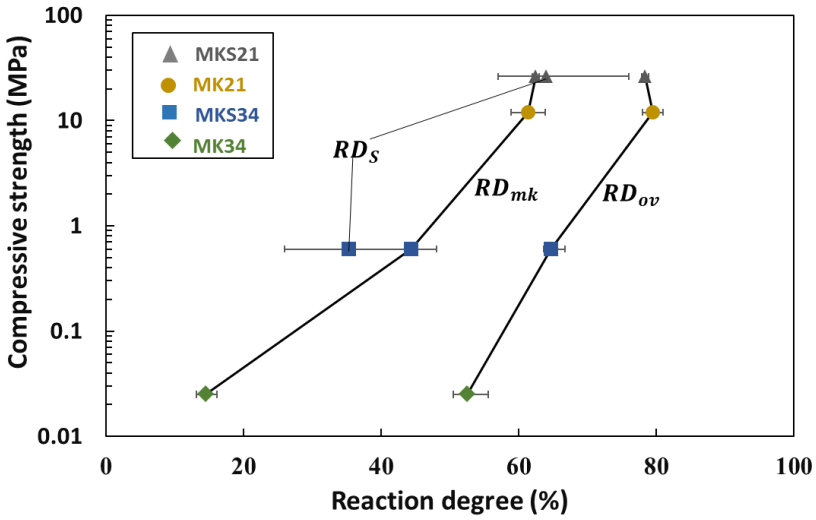

Figure 10. Compressive strength versus the degree of reaction at 28 days

4. General discussion

The studied materials cover a range of compositions and properties where H_2O/Na_2O varies from 21 to 34 and the slag proportion from 0 to 25% as a replacement of metakaolin. Increasing water content has been reported to induce changes in the kinetics of the process and the composition and nanostructure of the reaction products [29] [8] [9]. N-A-S-H precipitated with various types of zeolite related generally to low strength materials as reported in [35], however they were not detected in the present study through XRD. ^{27}Al and ^{29}Si MAS NMR spectroscopy, which provide further insight into the amorphous structure of the product phase, showed that the variation of H_2O/Na_2O ratio would not change the type of product formed in activated metakolin and binary mixtures. Therefore, the drop in compressive strength with higher H_2O/Na_2O can be attributed to the influence on the

reactivity of the precursor and the lower fraction of binding phase rather than the change of products composition or zeolite phase formation in the range of molar ratios studied in this work.

NMR results showed that the main reaction product in activated metakaolin system is the so-called geopolymer gel N-A-S-H regardless the H_2O/Na_2O ratio; its fraction increased with reaction time especially at high H_2O/Na_2O ratio. Regarding the product phase in binary mixtures, different methods have been exposed and implemented taking into account the different approaches found in the literature. ^{29}Si spectra of binary mixtures shifted to higher frequencies than plain metakaolin based material. Method 2 proves that the distinction of two phases attributed respectively to the conventional C-A-S-H (higher frequencies) and the 3D polymerized network (lower frequencies) does not represent the real phase composition. This is due to the modified phase formed at lower frequencies which does not represent the geopolymer structure obtained in a plain metakaolin mixture. Besides, method 2-bis confirmed the formation of a phase that lies between higher and lower frequencies. Chen et al. [26] [38] have attributed this phase to the contribution of both C-A-S-H phase with chain structures and calcium-modified geopolymer (Ca,Na)-A-S-H with a three-dimensional structure. Another study suggested the possibility for Q^2 and q^4 species to belong to the same phase in contradiction with the structure of both 3D network and C-A-S-H [55].

Method 3 concurred with the conclusion of method 2. It was based on the proposed peak positions in the ^{29}Si spectrum of an intermixed N-A-S-H and N-(C)-A-S-H both with 3D network structure [27]. At low pH value (<12), Ca-exchanged N-A-S-H appear to give (N, C)-A-S-H by ion exchange until all Na has been replaced by Ca which retain its 3D aluminosilicate framework. (N, C)-A-S-H exists at a pH<12 value and within the range of composition limits Na/Al<1.85 and Ca/Si<0.3 which is compatible with our initial composition (Na/Al=1 and Ca/Si =0.21) [17]. However, this method neglects the existence of

complex phases (presence of Q^2 and Q^3), which are not considered in the analysis. The peaks were chosen to define mainly a 3D structure with Q^4 Si species. In other words, we cannot exclude the possibility of the presence of Q^3 and Q^3(1Al) or the presence of a transitional phase between C-A-S-H and N-A-S-H expected to coexist in such systems, which implies the limit related to the deconvolution method.

Based on these interpretations, a conceptual model of the process can be proposed. The evolution of the polymerized network towards a well-defined C-A-S-H goes through the formation of a heterogeneous phase involved in the transformation of the 3D network to C-A-S-H. This heterogeneous phase can be supported by the presence of local structures at high and low frequencies, which are linked by q^4 Al species. The evolution of ^{29}Si spectra of the binary mixtures (Figure 11) especially the ^{29}Si spectra of the mixture MKS34 after a long time (after 500 days) confirms the suggested process model. The main resonance peak observed at 28 and 250 days on the ^{29}Si spectra widened after 500 days and a peak at -86 ppm started to appear as in the case of MKS21. This peak can be linked to the formation of Q^2 species in C-A-S-H. However, the ^{27}Al spectra do not show any remarkable evolution after 500 days compared to 28 and 250 days for the two mixtures MKS21 and MKS34 (Figure A. 1 in Appendix). Once again, these results shows that the same phase is formed in the two mixtures with a delayed evolution due to the effect of water. In addition, the evolution between ^{29}Si spectra of the mixture MKS21 at 250 days and after 500 days may suggest the possible stability of this phase.

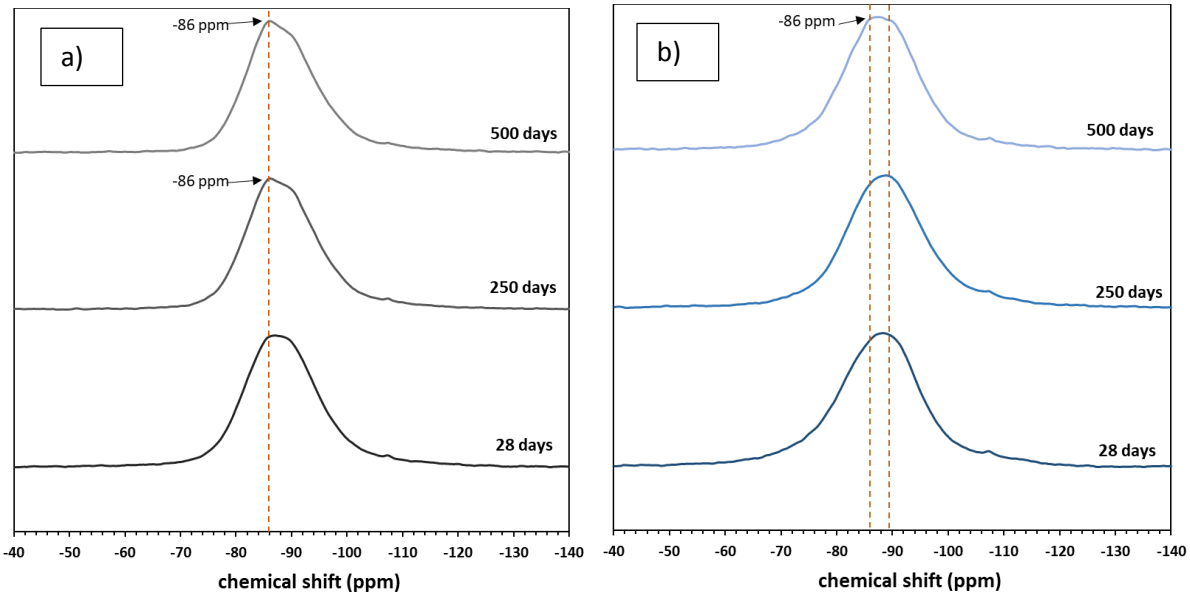

Figure 11. ^{29}Si MAS NMR spectra of activated metakaolin-slag systems (a) MKS21 (b) MKS34 at 28, 250, and 500 days

Finally, the evaluation of the reaction degree showed that adding slag to the mixture increased the reactivity of metakaolin and resulted in higher compressive strength in comparison to plain metakaolin mixtures. However, plain metakaolin and binary mixtures showed similar behavior about the drop in compressive strength at high H_2O/Na_2O.

5. Conclusion

In this article, different approaches, based on the different opinions evoked in the literature, were discussed to explore the phase composition in binary activated metakaolin mixtures with 25% of slag, by comparison with plain metakaolin mixtures. The influence of the incorporation of calcium on the local structure was investigated. The effect of H_2O/Na_2O ratio, which is a key parameter to design alkali-activated materials, was also studied. The following conclusions can be drawn from experimental results and their analysis:

- The challenge of the decomposition methods lied in the representation of the products, however they agreed with each other in term of reaction degree. A particular attention

should be paid to the use of the deconvolution method, as different peaks could be present at the same chemical shifts thus some will be neglected.

- The analysis of the phase composition of a mixture containing 25% of slag and 75 % of metakaolin as precursors suggested the presence of a heterogeneous phase involved in the transformation of 3D network to C-A-S-H , supporting the presence of local structures at high and low frequencies, which are linked by q^4 Al species. This suggestion is based on the comparison of different approaches.
- Increasing H_2O/Na_2O ratio in plain and binary mixtures resulted in higher content of unreacted precursors and a lower product fraction without changing the local structure of products, which can explain the drop in the compressive strength as H_2O/Na_2O increased.
- Adding slag to the mixture increased the reactivity of metakaolin and resulted in higher compressive strength in comparison with plain metakaolin mixtures.

Finally, it seems interesting to study the durability and the ion transport properties of these materials, which are partly controlled by gel nanostructure.

CRediT authorship contribution statement

F. Souayfan: Investigation, formal analysis, writing - original draft;
E. Rozière: Supervision, formal analysis, writing - review & editing;
M. Paris: Investigation, formal analysis, writing – review & editing;
D. Deneele: Investigation, formal analysis,
A. Loukili: Funding acquisition, supervision,
C. Justino: Funding acquisition, supervision

Acknowledgements

Funding: The authors would like to acknowledge financial and technical support of Soletanche Bachy France.

Declaration of Competing Interest

The authors declare that they have no known competing financial interests or personal relationships that could have appeared to influence the work reported in this paper.

References

[1] H. Güllü et A. Ali Agha, « The rheological, fresh and strength effects of cold-bonded geopolymer made with metakaolin and slag for grouting », *Construction and Building Materials*, vol. 274, p. 122091, mars 2021, doi: 10.1016/j.conbuildmat.2020.122091.

[2] H. Güllü, M. M. D. Al Nuaimi, et A. Aytek, « Rheological and strength performances of cold-bonded geopolymer made from limestone dust and bottom ash for grouting and deep mixing », *Bull Eng Geol Environ*, oct. 2020, doi: 10.1007/s10064-020-01998-2.

[3] A. Hassan, M. Arif, et M. Shariq, « Use of geopolymer concrete for a cleaner and sustainable environment – A review of mechanical properties and microstructure », *Journal of Cleaner Production*, vol. 223, p. 704‑728, juin 2019, doi: 10.1016/j.jclepro.2019.03.051.

[4] Y. Wu, B. Lu, Z. Yi, F. Du, et Y. Zhang, « The Properties and Latest Application of Geopolymers », *IOP Conf. Ser.: Mater. Sci. Eng.*, vol. 472, p. 012029, févr. 2019, doi: 10.1088/1757-899X/472/1/012029.

[5] J. L. Provis, « Geopolymers and other alkali activated materials: why, how, and what? », *Mater Struct*, p. 15, 2014, doi: 10.1617/s11527-013-0211-5.

[6] R. J. Myers, S. A. Bernal, R. San Nicolas, et J. L. Provis, « Generalized Structural Description of Calcium–Sodium Aluminosilicate Hydrate Gels: The Cross-Linked Substituted Tobermorite Model », *Langmuir*, vol. 29, n° 17, p. 5294‑5306, 2013, doi: 10.1021/la4000473.

[7] I. G. Richardson, « The calcium silicate hydrates », *Cement and Concrete Research*, vol. 38, n° 2, p. 137‑158, févr. 2008, doi: 10.1016/j.cemconres.2007.11.005.

[8] K. Scrivener, F. Martirena, S. Bishnoi, et S. Maity, « Calcined clay limestone cements (LC3) », *Cement and Concrete Research*, vol. 114, p. 49‑56, déc. 2018, doi: 10.1016/j.cemconres.2017.08.017.

[9] A. Fernandez-Jimenez, I. García-Lodeiro, et A. Palomo, « Durability of alkali-activated fly ash cementitious materials », *J Mater Sci*, vol. 42, n° 9, p. 3055‑3065, mai 2007, doi: 10.1007/s10853-006-0584-8.

[10] R. Pouhet et M. Cyr, « Studies of Natural and Accelerated Carbonation in Metakaolin-Based Geopolymer », *AST*, vol. 92, p. 38‑43, oct. 2014, doi: 10.4028/www.scientific.net/AST.92.38.

[11] M. Zhang, M. Zhao, G. Zhang, P. Nowak, A. Coen, et M. Tao, « Calcium-free geopolymer as a stabilizer for sulfate-rich soils », *Applied Clay Science*, vol. 108, p. 199‑207, mai 2015, doi: 10.1016/j.clay.2015.02.029.

[12] S. Rios, C. Ramos, A. Viana da Fonseca, N. Cruz, et C. Rodrigues, « Mechanical and durability properties of a soil stabilised with an alkali-activated cement », *European Journal of Environmental and Civil Engineering*, vol. 23, n° 2, p. 245‑267, févr. 2019, doi: 10.1080/19648189.2016.1275987.

[13] N. B. Singh et B. Middendorf, « Geopolymers as an alternative to Portland cement: An overview », *Construction and Building Materials*, vol. 237, p. 117455, mars 2020, doi: 10.1016/j.conbuildmat.2019.117455.
[14] L. K. Turner et F. G. Collins, « Carbon dioxide equivalent (CO2-e) emissions: A comparison between geopolymer and OPC cement concrete », *Construction and Building Materials*, vol. 43, p. 125‑130, juin 2013, doi: 10.1016/j.conbuildmat.2013.01.023.
[15] *Handbook of Alkali-Activated Cements, Mortars and Concretes*. Elsevier, 2015. doi: 10.1016/C2013-0-16511-7.
[16] A. Cherki El Idrissi, M. Paris, E. Rozière, D. Deneele, S. Darson, et A. Loukili, « Alkali-activated grouts with incorporated fly ash: From NMR analysis to mechanical properties », *Materials Today Communications*, vol. 14, p. 225‑232, mars 2018, doi: 10.1016/j.mtcomm.2018.01.012.
[17] I. Garcia-Lodeiro, A. Palomo, A. Fernández-Jiménez, et D. E. Macphee, « Compatibility studies between N-A-S-H and C-A-S-H gels. Study in the ternary diagram Na2O–CaO–Al2O3–SiO2–H2O », *Cement and Concrete Research*, vol. 41, n° 9, p. 923‑931, sept. 2011, doi: 10.1016/j.cemconres.2011.05.006.
[18] S. A. Bernal, J. L. Provis, V. Rose, et R. Mejía de Gutierrez, « Evolution of binder structure in sodium silicate-activated slag-metakaolin blends », *Cement and Concrete Composites*, vol. 33, n° 1, p. 46‑54, janv. 2011, doi: 10.1016/j.cemconcomp.2010.09.004.
[19] S. A. Bernal, E. D. Rodríguez, R. Mejía de Gutiérrez, M. Gordillo, et J. L. Provis, « Mechanical and thermal characterisation of geopolymers based on silicate-activated metakaolin/slag blends », *J Mater Sci*, vol. 46, n° 16, p. 5477‑5486, août 2011, doi: 10.1007/s10853-011-5490-z.
[20] A. Buchwald, H. Hilbig, et Ch. Kaps, « Alkali-activated metakaolin-slag blends—performance and structure in dependence of their composition », *J Mater Sci*, vol. 42, n° 9, p. 3024‑3032, mai 2007, doi: 10.1007/s10853-006-0525-6.
[21] S. A. Bernal, « Effect of the activator dose on the compressive strength and accelerated carbonation resistance of alkali silicate-activated slag/metakaolin blended materials », *Construction and Building Materials*, vol. 98, p. 217‑226, nov. 2015, doi: 10.1016/j.conbuildmat.2015.08.013.
[22] O. Burciaga-Díaz, R. X. Magallanes-Rivera, et J. I. Escalante-García, « Alkali-activated slag-metakaolin pastes: strength, structural, and microstructural characterization », *Journal of Sustainable Cement-Based Materials*, p. 18, 2013, doi: 10.1080/21650373.2013.801799.
[23] O. Burciaga-Díaz, J. I. Escalante-García, R. Arellano-Aguilar, et A. Gorokhovsky, « Statistical Analysis of Strength Development as a Function of Various Parameters on Activated Metakaolin/Slag Cements », *Journal of the American Ceramic Society*, vol. 93, n° 2, p. 541‑547, févr. 2010, doi: 10.1111/j.1551-2916.2009.03414.x.
[24] G. Samson, M. Cyr, et X. X. Gao, « Formulation and characterization of blended alkali-activated materials based on flash-calcined metakaolin, fly ash and GGBS », *Construction and Building Materials*, vol. 144, p. 50‑64, juill. 2017, doi: 10.1016/j.conbuildmat.2017.03.160.
[25] A. Hasnaoui, E. Ghorbel, et G. Wardeh, « Optimization approach of granulated blast furnace slag and metakaolin based geopolymer mortars », *Construction and Building Materials*, vol. 198, p. 10‑26, févr. 2019, doi: 10.1016/j.conbuildmat.2018.11.251.
[26] X. Chen, A. Sutrisno, et L. J. Struble, « Effects of calcium on setting mechanism of metakaolin-based geopolymer », *Journal of the American Ceramic Society*, p. 12, 2017, doi: 10.1111/jace.15249.
[27] P. Perez-Cortes et J. I. Escalante-Garcia, « Gel composition and molecular structure of alkali-activated metakaolin-limestone cements », *Cement and Concrete Research*, p. 13, 2020, doi: 10.1016/j.cemconres.2020.106211.
[28] B. Walkley et J. L. Provis, « Solid-state nuclear magnetic resonance spectroscopy of cements », *Materials Today Advances*, vol. 1, p. 100007, mars 2019, doi: 10.1016/j.mtadv.2019.100007.
[29] C. Ruiz-Santaquiteria, J. Skibsted, A. Fernández-Jiménez, et A. Palomo, « Alkaline solution/binder ratio as a determining factor in the alkaline activation of aluminosilicates », *Cement and Concrete Research*, p. 10, 2012, doi: 10.1016/j.cemconres.2012.05.019.

[30] A. Aboulayt *et al.*, « Alkali-activated grouts based on slag-fly ash mixtures: From early-age characterization to long-term phase composition », *Construction and Building Materials*, vol. 260, p. 120510, nov. 2020, doi: 10.1016/j.conbuildmat.2020.120510.

[31] F. Cassagnabère, P. Diederich, M. Mouret, G. Escadeillas, et M. Lachemi, « Impact of metakaolin characteristics on the rheological properties of mortar in the fresh state », *Cement and Concrete Composites*, vol. 37, p. 95‑107, mars 2013, doi: 10.1016/j.cemconcomp.2012.12.001.

[32] P. Duxson, A. Fernández-Jiménez, J. L. Provis, G. C. Lukey, A. Palomo, et J. S. J. van Deventer, « Geopolymer technology: the current state of the art », *J Mater Sci*, vol. 42, nº 9, p. 2917‑2933, mai 2007, doi: 10.1007/s10853-006-0637-z.

[33] A. Cherki El Idrissi, « The development of a global mix design and analysis approach for alkali activated soil reinforcement grouts », *European Journal of Environmental and Civil Engineering*, vol. 23, nº 5, p. 645‑656, mai 2019, doi: 10.1080/19648189.2018.1519461.

[34] M. Lizcano, A. Gonzalez, S. Basu, K. Lozano, et M. Radovic, « Effects of Water Content and Chemical Composition on Structural Properties of Alkaline Activated Metakaolin-Based Geopolymers », *J. Am. Ceram. Soc.*, vol. 95, nº 7, p. 2169‑2177, juill. 2012, doi: 10.1111/j.1551-2916.2012.05184.x.

[35] V. Benavent, F. Frizon, et A. Poulesquen, « Effect of composition and aging on the porous structure of metakaolin-based geopolymers », *J Appl Crystallogr*, vol. 49, nº 6, p. 2116‑2128, déc. 2016, doi: 10.1107/S1600576716014618.

[36] K. Juengsuwattananon, F. Winnefeld, P. Chindaprasirt, et K. Pimraksa, « Correlation between initial SiO2/Al2O3, Na2O/Al2O3, Na2O/SiO2 and H2O/Na2O ratios on phase and microstructure of reaction products of metakaolin-rice husk ash geopolymer », *Construction and Building Materials*, vol. 226, p. 406‑417, nov. 2019, doi: 10.1016/j.conbuildmat.2019.07.146.

[37] K. Juengsuwattananon et K. Pimraksa, « VARIABLE FACTORS CONTROLLING AMORPHOUS-ZEOLITE PHASE TRANSFORMATION IN METAKAOLIN BASED GEOPOLYMER », *Acta Metall Slovaca*, vol. 23, nº 4, p. 378‑386, déc. 2017, doi: 10.12776/ams.v23i4.1001.

[38] X. Chen, E. Kim, P. Suraneni, et L. Struble, « Quantitative Correlation between the Degree of Reaction and Compressive Strength of Metakaolin-Based Geopolymers », *Materials*, vol. 13, nº 24, p. 5784, déc. 2020, doi: 10.3390/ma13245784.

[39] Z. Sun et A. Vollpracht, « Isothermal calorimetry and in-situ XRD study of the NaOH activated fly ash, metakaolin and slag », *Cement and Concrete Research*, vol. 103, p. 110‑122, janv. 2018, doi: 10.1016/j.cemconres.2017.10.004.

[40] B. Walkley *et al.*, « Phase evolution of C-(N)-A-S-H/N-A-S-H gel blends investigated via alkali-activation of synthetic calcium aluminosilicate precursors », *Cement and Concrete Research*, vol. 89, p. 120‑135, nov. 2016, doi: 10.1016/j.cemconres.2016.08.010.

[41] I. Sobrados et J. Sanz, « A´ ngel Palomo, Santiago Alonso, and Ana Fernandez-Jime´nez », *Journal of the American Ceramic Society*, vol. 87, nº 6, p. 5, 2004.

[42] J. Davidovits, « GEOPOLYMERS: Man-Made Rock Geosynthesis and the Resulting Development of Very Early High Strength Cement », p. 25.

[43] C. Li, H. Sun, et L. Li, « A review: The comparison between alkali-activated slag (Si+Ca) and metakaolin (Si+Al) cements », *Cement and Concrete Research*, vol. 40, nº 9, p. 1341‑1349, sept. 2010, doi: 10.1016/j.cemconres.2010.03.020.

[44] B. Walkley, X. Ke, O. H. Hussein, S. A. Bernal, et J. L. Provis, « Incorporation of strontium and calcium in geopolymer gels », *Journal of Hazardous Materials*, vol. 382, p. 121015, janv. 2020, doi: 10.1016/j.jhazmat.2019.121015.

[45] I. Garcı´a-Lodeiro, A. Ferna´ndez-Jime´nez, A. Palomo, et D. E. Macpheey, « Effect of Calcium Additions on NASH Cementitious Gels », *Journal of the American Ceramic Society*, vol. 93, nº 7, p. 7, 2010, doi: 10.1111/j.1551-2916.2010.03668.x.

[46] S. A. Bernal *et al.*, « Gel nanostructure in alkali-activated binders based on slag and fly ash, and effects of accelerated carbonation », *Cement and Concrete Research*, vol. 53, p. 127‑144, nov. 2013, doi: 10.1016/j.cemconres.2013.06.007.

[47] D. Massiot *et al.*, « Modelling one- and two-dimensional solid-state NMR spectra: Modelling 1D and 2D solid-state NMR spectra », *Magn. Reson. Chem.*, vol. 40, n° 1, p. 70‑76, janv. 2002, doi: 10.1002/mrc.984.
[48] S. Puligilla et P. Mondal, « Co-existence of aluminosilicate and calcium silicate gel characterized through selective dissolution and FTIR spectral subtraction », *Cement and Concrete Research*, p. 11, 2015, doi: 10.1016/j.cemconres.2015.01.006.
[49] G. Engelhardt, « Multinuclear solid-state NMR in silicate and zeolite chemistry », *TrAC Trends in Analytical Chemistry*, vol. 8, n° 9, p. 343‑347, oct. 1989, doi: 10.1016/0165-9936(89)87043-8.
[50] A. Buchwald, « Condensation of aluminosilicate gels—model system for geopolymer binders », *Journal of Non-Crystalline Solids*, p. 7, 2011, doi: https://doi.org/10.1016/j.jnoncrysol.2010.12.036.
[51] R. J. Myers, E. L'Hôpital, J. L. Provis, et B. Lothenbach, « Effect of temperature and aluminium on calcium (alumino)silicate hydrate chemistry under equilibrium conditions », *Cement and Concrete Research*, vol. 68, p. 83‑93, févr. 2015, doi: 10.1016/j.cemconres.2014.10.015.
[52] S. Puligilla et P. Mondal, « Role of slag in microstructural development and hardening of fly ash-slag geopolymer », *Cement and Concrete Research*, vol. 43, p. 70‑80, janv. 2013, doi: 10.1016/j.cemconres.2012.10.004.
[53] J. Temuujin, A. van Riessen, et R. Williams, « Influence of calcium compounds on the mechanical properties of fly ash geopolymer pastes », *Journal of Hazardous Materials*, vol. 167, n° 1‑3, p. 82‑88, août 2009, doi: 10.1016/j.jhazmat.2008.12.121.
[54] X. Chen, A. Sutrisno, L. Zhu, et L. J. Struble, « Setting and nanostructural evolution of metakaolin geopolymer », *J Am Ceram Soc*, vol. 100, n° 5, p. 2285‑2295, mai 2017, doi: 10.1111/jace.14641.
[55] E. Coudert, M. Paris, D. Deneele, G. Russo, et A. Tarantino, « Use of alkali activated high-calcium fly ash binder for kaolin clay soil stabilisation: Physicochemical evolution », *Construction and Building Materials*, vol. 201, p. 539‑552, mars 2019, doi: 10.1016/j.conbuildmat.2018.12.188.

Appendix

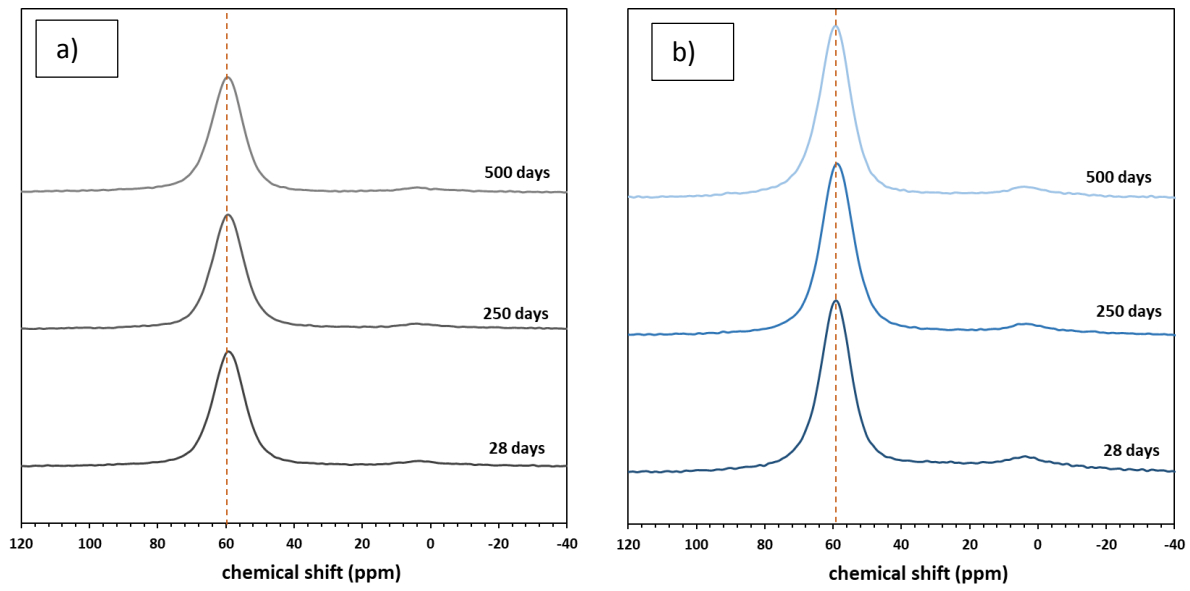

Figure A. 1 ^{27}Al MAS NMR spectra of activated metakaolin-slag systems (a) MKS21 (b) MKS34 at 28, 250, and 500 days

Manuscript Number: CONBUILDMAT-D-21-08563

Title: Apply ^{29}Si and ^{27}Al MAS NMR in identifying the phase composition and the reaction degree of alkali activated metakaolin-slag mixtures based on review and experimental study

Faten Souayfan, Emmanuel Rozière, Michaël Paris, Dimitri Deneele, Ahmed Loukili, Christophe Justino

Authors answers:

The authors would like to thank the reviewers for their efforts in handling this scientific work. The interesting remarks are gratefully acknowledged and will definitely improve the quality of this paper. All comments and suggestions have been addressed in the new version of the manuscript. The modifications are marked in orange characters in the revised manuscript to facilitate the review process. The table below presents the changes performed and responses to the reviewers' comments and recommendations, in the order they were raised.

Reviewer #1:

Paper appears to be good and authors have tried to investigate the composition of the reaction product and degree of reaction.

The title should be modified as: ^{29}Si and ^{27}Al MAS NMR spectroscopic studies of activated metakaolin-slag mixtures	The authors thank reviewer's helpful suggestion. The title have been modified as recommended.
English requires improvement	Some parts of the text have been corrected, removed, or rewritten. The new Results and discussion part is one page shorter at equivalent content (not taking into account the new text).
Interpretations should be concise	
Based on the findings, author should propose a conceptual model for the entire process	In this context, a part in the discussion section has been added, with new data related to long-term behavior to support the statements.

Reviewer #2:

It was unclear how to obtain amorphous fraction of metakaolin and slag and no report on the amorphous content of slag.	The amorphous fraction of metakaolin (53%) was deduced from XRD analyses [1]. XRD analysis of slag only showed an amorphous hump thus it was mainly composed of amorphous phases. The molar ratios of studied mixtures were determined taking into account the amorphous part of metakaolin and the overall composition of slag.
It was unclear to report Si/Al in Table 2. It was atomic ratio or mole ratio of oxides in term of SiO_2/Al_2O_3.	The texte has been modified and Table 2 has been updated to make it clearer.

Please recheck Na-silicate, dispersant and water used in MK34 in Table 2. Were they 3.0, 367 and 0.75, respectively?	The compositions of MK21 and MK34 have been checked and updated in Table 2.
Please clarify what was the difference between NaOH and total NaOH in activating solution. Why MK34 that used the highest NaOH content showed the lower total NaOH in activating solution in Table 2.	Silicate solution used in this study provides a SiO_2/Na_2O molar ratio (modulus) of 1.7 and 44wt% of dry matter. This molar ratio is much lower than most existing sodium silicate activators. Commercial sodium silicate solution generally have a modulus around 3. The activator used in this study is equivalent to a sodium silicate solution of modulus of 3 mixed with a 5M NaOH solution (for MK21 mixture). The sodium silicate solution used in this study has been especially designed by the provider with higher initial Na_2O content to minimize adding NaOH during the preparation of grouts, as the dissolution of NaOH in water can be a hazardous operation. A small amount of NaOH was added in pellets to adjust the Na/Al molar ratio. The total NaOH in activating solution includes equivalent NaOH from the sodium silicate solution deduced from the Na_2O molar content, and NaOH in pellets as mentioned in the text in this section. A clarification has been added also in the text : *The total NaOH content in activating solution includes NaOH from the sodium silicate solution deduced from its Na_2O molar content, and NaOH in pellets*
In the part of 3.2.1, calcite was seen in MK in almost the same intensity in MKS. It was quite unreasonable. Why MKS that contained higher CaO content showed almost the same value?	Authors agree with the reviewer that it primary appears unreasonable to detect calcite in MK and MKS at almost the same intensity. It is noteworthy to mention that only the crystalline fraction of calcite in metakaolin/slag can be detected, thus it is not obvious to correlate intensity in XRD patterns and actual calcite contents in the samples. The raw metakaolin contained calcite. Only the sample MK21 analyzed at 28 days showed significant calcite peak. This mixture actually had the highest initial metakaolin content. The peak was not observed at 250 days, probably due to the consumption of calcite. In binary mixtures, the formation of calcite can be favored due to the higher initial calcium content but on the other hand calcium can be incorporated in the reaction products. Calcite

	can thus form from the carbonation of hydration products. Therefore, it seems difficult to predict the intensity of calcite in analyses as it influenced by many factors.
In Fig. 2, kaolinite peaks were hardly seen but the explanation reported the existence. It would be helpful to show XRD of the starting metakaolin if kaolinite was still present before activation.	The authors confirm the presence of kaolinite peak in raw metakaolin. XRD patterns of raw metakoalin and slag have been added in Figure 2.
The hump peaks as mentioned both at 25-35 and 30 of two theta in Fig.2 were difficult to be noticed. It would be helpful to magnify the hump peaks for more understanding.	The hump has been magnified and added in Figure 2.
In the part of 3.2.2, author only explained the shift of spectrum in Fig. 3 according to the difference in starting materials (with and without slag) but not yet the elaborating in different H_2O/N_2O ratios.	The main difference due to the variation of H_2O/Na_2O lies in spectral intensity below 40 ppm (Al^V and Al^{VI} signals). This is mentioned in the text. The H_2O/Na_2O ratio did not significantly influence the main peak position. It has been added in the text for more clarification : *The variation of H_2O/Na_2O did not significantly influence the position of the main resonance peak in both types of mixtures.*
In the part of 3.2.2, in Fig. 4, the explanation on the development of Q type (0-4) should be added as comparison in differences of H_2O/N_2O and with/without slag mixtures.	Comparison in differences of H_2O/Na_2O and with/without slag **has been inserted in the text**. The explanation of these shifts is more detailed in the next section where the decomposition method allowed understanding the differences in Si spectra as a function of different parameters.
In the part of 3.2.2 according to Table 4 & Fig.5, in page 17 (line 1-17), it was not true to report that geopolymer structure is formed whatever H_2O/N_2O ratio as confirmed by the very low compressive strength.	As RMN allows exploring the local structure, the shifts in Al spectra and the Si spectra are in accordance with the formation of a geopolymer structure in these mixtures. It was shown in this part that a geopolymer structure was formed whatever the H_2O/Na_2O ratio but with lower proportion at high H_2O/Na_2O ratio. In other words, the low compressive strength does not mean that the geopolymer is not formed, it is formed but with a much lower proportion. As mentioned in the discussion part, the drop in compressive strength with higher H_2O/Na_2O can be attributed to the influence on the reactivity of the precursor and the lower fraction of binding phase

	rather than the change of products composition.
In Fig.8 & Table 6, it was unclear to report that increasing H_2O/Na_2O ratio resulted in a slight increase in Si/Al that was contradict to the previous part mentioning high H_2O/Na_2O contained higher unreacted part. Also, the starting Si/Al ratios of MKS21 and MKS34 were kept the similar values.	The Si/Al ratio was calculated by taking into account the binding phase without the contribution of raw materials. The slight increase in Si/Al ratio is due to a lower amount of Al dissolved at higher H_2O/Na_2O so Si/Al is higher. On the other hand, the trend of the variation of Si/Al as a function of time is not clear. This underlines once again the issues related to the deconvolution method.
In page 22, line 53-57, it was not all true to report that the increase in mechanical properties at lower Si/Al. What was the basis of lower Si/Al? In which part of this research that was relevant to increasing in strength at lower Si/Al ratio.	The lower Si/Al ratio at lower H_2O/Na_2O is attributed to the higher amount of AlO_4 coordinated due to a higher dissolution of precursors. The authors agree that the correlation between Si/Al and the mechanical properties is not obvious. Moreover, linking the variations of Si/Al and mechanical properties was not the purpose of the analysis. This part has been removed. The authors prefer highlighting the limitations related to the deconvolution method and discussing the validity of the Si/Al ratio in this part.
Please recheck the writing of species used for orthosilicic acid in page 23 (line 1-8).	The formula has been corrected. However, it has been removed from the text.
The explanations on reaction degree according to Table 7 and Fig.9 might lead to misunderstanding in term of H_2O/Na_2O of 34 in both mixtures that showed not so much difference in overall reaction degree from H_2O/N_2O of 21 but their strength was greatly different.	The overall reaction degree as well the reactivity of raw materials were remarkably influenced by the H_2O/Na_2O ratio. The reaction degree decreases from 80 % to 54 % and from 80 to 67% by increasing the H_2O/Na_2O ratio in MK and MKS mixtures respectively. In addition, as reported in Figure 9, the compressive strength cannot be just explained by the reaction degree alone, it is also affected by microstructural parameters and the fraction of solid phase, which mainly depends on initial solid fraction and chemically bound water content. This has been mentioned in the text.

Please, find attached a revised version of our manuscript. We hope these answers will meet your expectations and that the processing of this paper will resume normally.

Sincerely

[1] F. Cassagnabère, P. Diederich, M. Mouret, G. Escadeillas, et M. Lachemi, « Impact of metakaolin characteristics on the rheological properties of mortar in the fresh state », *Cement and Concrete Composites*, vol. 37, p. 95‑107, mars 2013, doi: 10.1016/j.cemconcomp.2012.12.001.

Highlights

- Activated metakaolin and metakaolin-slag mixtures studied at high H_2O/Na_2O ratios
- Different approaches of Si and Al NMR spectra analysis are compared
- Formation of a heterogeneous phase involved in the transformation of 3D geopolymer network to C-A-S-H
- Higher reactivity of metakaolin detected in slag-metakaolin mixtures

CRediT authorship contribution statement

F. Souayfan: Investigation, formal analysis, writing - original draft;

E. Rozière: Supervision, formal analysis, writing - review & editing;

M. Paris: Investigation, formal analysis, writing – review & editing;

D. Deneele: Investigation, formal analysis,

A. Loukili: Funding acquisition, supervision,

C. Justino: Funding acquisition, supervision

^{29}Si and ^{27}Al MAS NMR spectroscopic studies of activated metakaolin-slag mixtures

Faten Souayfan[a], Emmanuel Rozière[a], Michaël Paris[b], Dimitri Deneele[b,c], Ahmed Loukili[a], Christophe Justino [d]

[a] Civil engineering and Mechanics Research Institute (GeM), UMR-CNRS 6183, Ecole Centrale de Nantes, 1 rue de la Noe – 44321 Nantes, France

[b] Université de Nantes, CNRS, Institut des Matériaux Jean Rouxel, IMN, F-44000 Nantes, France

[c] GERS-LGIE, Université Gustave Eiffel, IFSTTAR, F-44344 Bouguenais, France

[d] Soletanche-Bachy, Chemin des Processions – 77130 Montereau Fault Yonne, France

Abstract

Blending metakaolin with slag in alkali-activated materials represents a promising way to achieve both acceptable engineering properties and durability. Nuclear Magnetic Resonance (NMR) spectroscopy has appeared as a key technique to investigate the structure of alkali-activation products. However, there is not a consensus on the analysis of NMR spectra to identify the phases formed in binary slag-metakaolin mixtures. This paper characterizes the phase composition and the reaction degree of alkali-activated metakaolin-slag blends, with special emphasis on the effect of H_2O/Na_2O ratio. Different approaches based on the literature are presented and implemented to analyze NMR data. The results suggest the formation of a heterogeneous phase involved in the transformation of 3D network to C-A-S-H. The evaluation of the reaction degree showed that the incorporation of slag in activated metakaolin mixtures resulted in higher reactivity of metakaolin and higher compressive strength.

Keywords

Alkali activated materials, Metakaolin, Slag, Sodium silicate Reaction degree, ^{29}Si MAS NMR, ^{27}Al MAS NMR, Geopolymer, Strength

Declaration of interests

☒ The authors declare that they have no known competing financial interests or personal relationships that could have appeared to influence the work reported in this paper.

☐The authors declare the following financial interests/personal relationships which may be considered as potential competing interests: